AD-A181 414 LONG NONLINEAR WAVES IN THE LOWER ATMOSPHERE(U) 1/1
AUSTRALIAN NATIONAL UNIV CANBERRA RESEARCH SCHOOL OF
EARTH SCIENCES D R CHRISTIE 06 MAY 87 87-1
UNCLASSIFIED AFOSR-TR-87-0780 AFOSR-83-0045 F/G 4/2 NL

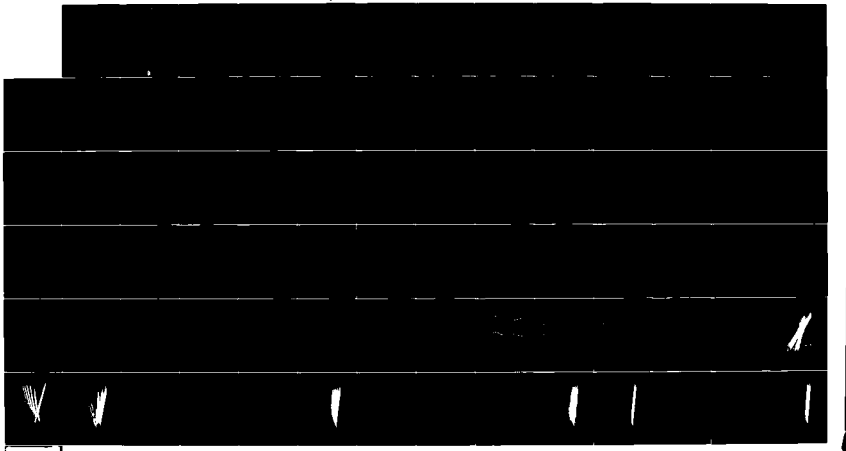

END
DATE
FILMED
7-87

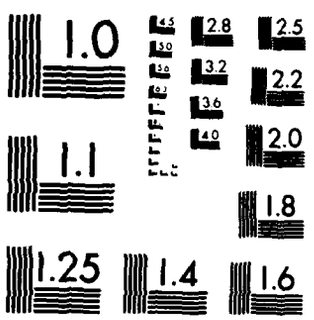

(2)

REPORT DOCUMENTATION PAGE	READ INSTRUCTIONS BEFORE COMPLETING FORM
1. Report Number AFOSR-TR- 87-0780	2. Govt Accession No. / 3. Recipient's Catalog Number
4. Title (and Subtitle) Long Nonlinear Waves in the Lower Atmosphere	5. Type of Report & Period Covered: Final Scientific Report Period ending 31 December, 1985
	6. Performing Org. Report Number: 87-1
7. Author(s) D. R. Christie	8. Contract or Grant Number: AFOSR-83-0045
9. Performing Organization Name and Address: Research School of Earth Sciences, The Australian National University, P. O. Box 4, Canberra, ACT, Australia, 2600	10. Program Element, Project, Task Area & Work Unit Numbers: 61102f, 2309, A1
11. Controlling Office Name and Address: Air Force Office of Scientific Research, Building 410, Bolling Air Force Base, Washington, D. C. 20332-6448	12. Report Date: 6 May 1987 / 13. Number of Pages: 80
14. Monitoring Agency Name and Address: same as 11.	15.
16. & 17. Distribution Statement: Approved for public release; distribution unlimited.	
18. Supplementary Notes	
19. Key Words: Solitary Atmospheric Waves, Long Nonlinear Waves, Internal Bore Waves	

20. Abstract: A general theoretical treatment of long nonlinear wave propagation in the lower atmosphere is presented. The eigenvalue problem for finite-amplitude waves in a surface-based inversion is discussed in detail and expressions are obtained in closed form for the nonlinear wave parameters, surface perturbation pressure and wind components for a number of realistic boundary-layer waveguide models. The governing evolution equations for wave amplitude have been solved numerically for a wide variety of initial conditions and the results are found to compare favourably with observations. Nonlinear wave propagation in an inhomogeneous waveguide is also studied in detail. It is shown that both temporal and spatial variations in the degree of turbulent dissipation can induce significant changes in the speed of propagation and in the morphology of boundary-layer nonlinear wave disturbances.

FORM 1473

FINAL SCIENTIFIC REPORT

LONG NONLINEAR WAVES IN THE LOWER ATMOSPHERE

Prepared by

Douglas R. Christie
Research School of Earth Sciences
Australian National University

For

Air Force Office of Scientific Research
Bolling Air Force Base, DC 20332-6448

Grant Number AFOSR - 83 - 0045

6 May 1987

LONG NONLINEAR WAVES IN THE LOWER ATMOSPHERE

D.R. Christie

Research School of Earth Sciences

Australian National University

Canberra, A.C.T., 2601

ABSTRACT

This paper is concerned with the theoretical description of long, finite-amplitude waves in the stably-stratified lower atmosphere. The time evolution of these waves is governed to first order by the Benjamin-Davis-Ono (BDO) equation when frictional processes are negligible or by the BDO-Burgers equation when turbulent dissipation is significant. Numerical solutions of both of these model equations are presented for a wide variety of initial conditions ranging from long waves of finite volume to internal deep-fluid bore waves of infinite spatial extent. It is shown that initially smooth long wave disturbances evolve rapidly under ideal homogeneous waveguide conditions into solitary waves of exceptionally large amplitude. The BDO-Burgers equation is found to have highly stable time-independent deep-fluid internal bore wave solutions which may be either oscillatory or monotonic depending upon the degree of frictional dissipation. A number of specific models for the time evolution of long nonlinear atmospheric waves are proposed and discussed in detail. Explicit formulae are given for the wave propogation parameters, surface perturbation pressure, and wind components for three simple, but realistic, boundary layer inversion waveguides. A study has also been made of the influence on nonlinear wave propagation of either spatial or temporal variations in the degree of turbulent dissipation. It is shown that a sudden increase or decrease in the frictional damping coefficient, such as might be encountered at a land-sea boundary, can induce a significant variation in the speed of propagation and a substantial change in the morphology of finite-amplitude boundary layer wave disturbances. Finally, it is shown that wave induced turbulence plays an important role in the evolution of long nonlinear atmospheric waves.

1. Introduction

It has long been recognized that internal gravity waves are an important dynamical feature in the lower atmosphere. The significance of these ubiquitous waves arises from their ability to transfer energy and momentum and from the role they play in the generation of turbulence and in the initiation and organization of deep convection. In the last few years it has become increasingly clear that long gravity waves which propagate on inversions in the lower troposphere are often highly nonlinear in nature. A good illustration of the importance of nonlinearity in the description of long atmospheric wave disturbances is given by observations of solitary waves on nocturnal inversions over Northern Australia (Christie et al., 1978, 1979) and over Central Oklahoma (Doviak and Ge, 1984). Waves of this type often have amplitudes which are comparable to the effective depth of the inversion waveguide; they are an essentially nonlinear phenomenon and the successful description of their properties can only be given within the framework of nonlinear dispersive wave theory. Although linear long wave theory often provides a fairly good estimate of phase speed, an analysis based on the linearized equations completely fails to describe the morphology and evolution of finite-amplitude long internal wave disturbances. This paper will be concerned with a general theoretical description of nonlinear wave propagation in the stably-stratified lower atmosphere.

A particularly interesting and exceptionally well-documented example of nonlinear wave activity in the lower atmosphere is given by the 'morning glory' phenomenon of north-eastern Australia. The morning glory is a strong wind squall or series of wind squalls, often accompanied by one or more spectacular solitary wave roll cloud formations, occurring commonly near dawn with remarkable regularity during the spring months over the southern Gulf of Carpentaria region and the adjacent Cape York Peninsula. A number of observational studies carried out in recent years (Christie et al., 1981; Clarke et al., 1981; Christie and Muirhead, 1981, 1983 a,b; Smith

et al., 1982; Clarke, 1983b; Smith and Morton, 1984; Smith and Page, 1985; Smith et al. 1986) have shown that the morning glory is, in essence, a long nonlinear internal boundary-layer wave disturbance which evolves asymptotically in time into a family of large amplitude solitary waves. It is now widely recognised that similar large-amplitude propagating wave phenomena occur commonly, but usually without cloud, over much of the Australian region (Christie et al., 1978, 1979; Christie and Muirhead, 1983a, 1985; Drake 1984, 1985; Mulroney, 1984; Smith, 1986; Clarke, 1986; Physick, 1987) and elsewhere (Shreffler and Binkowski, 1981; Goncharov and Matveyev, 1982; Hasse and Smith, 1984; Doviak and Ge, 1984; additional references may be found in Christie and Muirhead, 1983b).

In the present paper we will be concerned with a general description of the evolution of morning glory waves and other closely-related nonlinear wave phenomena which are confined to the lower few kilometers of the atmosphere. Christie et al. (1978, 1979) proposed, on the basis of the atmospheric scales involved, that the evolution of boundary-layer disturbances of this type is governed, to first order, by the deep-fluid Benjamin-Davis-Ono (BDO) equation (Benjamin, 1967). Up until now, detailed theoretical modelling of atmospheric waves of this type has been limited largely to a study of the stationary solitary wave components. Solitary wave solutions of the BDO equation for a simple two-fluid boundary layer model were used by Christie et al. (1978) to interpret observations of nonlinear waves over the arid interior of northern Australia. A similar solitary wave analysis has been used by Goncharov and Matveyev (1982) to estimate the depth and intensity of boundary layer temperature inversions from nonlinear wave observations. Solitary wave solutions corresponding to a realistic analytical model for potential temperature and shear profiles in the ambient environment have been derived by Clarke et al. (1981) and compared with morning glory observations. Recently, Noonan and Smith (1985) have reported the results of a very detailed study of morning glory solitary waves based on a numerical treatment of the waveguide eigenvalue problem. In both of these latter investigations the

calculated morning glory wave speeds were found to compare favourably with observed propagation speeds. Clarke et al. found, however, that the predicted effective wavelengths of the solitary wave components were significantly smaller than those indicated by the observations, while in the investigation reported by Noonan and Smith, the predicted wavelengths were substantially larger than those observed.

It is assumed in all of these relatively simple model calculations that the time-independent Benjamin-Davis-Ono equation provides a valid description of these disturbances. Strictly speaking, the steady-state BDO equation is applicable only to completely non-interacting deep-fluid solitary waves of modest amplitude which propagate in an inviscid horizontally homogeneous waveguide embedded in a neutrally stable fluid of infinite extent. Since atmospheric solitary waves seldom, if ever, occur as effectively isolated phenomena independent of other solitary wave components, calculations of wave parameters based on the time-independent solutions of the BDO equation may be unreliable. Furthermore, the evolution of long nonlinear wave disturbances in the lower atmosphere is always subject to dissipative processes and may also be influenced by variations in waveguide structure. Thus, a more realistic description of these disturbances should be based on the time-dependent solution and should include the effects of spatial and temporal inhomogeneities in the waveguide structure, turbulent dissipation, and perhaps, damping due to the radiation of waves into the upper atmosphere. Since in many cases of interest the waveguide may be viewed as essentially uniform, the present paper will be primarily concerned with a theoretical study of the time-evolution of nonlinear wave disturbances under ideal homogeneous inviscid waveguide conditions and under conditions where turbulent dissipation plays a significant role in the evolution process.

A preliminary step in the study of the evolution of nonlinear boundary layer waves has been described by Christie and Muirhead (1981) who numerically solved the Benjamin-Davis-Ono equation for a variety of finite-volume initial long wave disturbances. Egger (1983, 1984) has also considered the development of morning

glory nonlinear waves in a simple two-fluid model based on the internal bore-wave solution of the classical shallow-fluid Korteweg-de Vries (KdV)-Burgers equation. It is clear, however, from the discussion in Benjamin (1967), that the Korteweg-de Vries equation does not provide a proper description of nonlinear waves in a surface-based waveguide beneath an unbounded fluid. This investigation will therefore focus on a study of the evolution of long nonlinear wave disturbances as given within the framework of a generalized deep-fluid Benjamin-Davis-Ono equation with turbulent dissipation.

A brief review of the observed properties of long nonlinear atmospheric wave disturbances as illustrated by the morning glory of the Gulf of Carpentaria is given in Section 2. This is followed in Section 3 by a discussion of the application of nonlinear dispersive wave theory to a description of finite-amplitude wave motions in the stably-stratified lower atmosphere. The Benjamin-Davis-Ono-Burgers equation is introduced at this point as a model equation for the dynamics of these nonlinear wave disturbances. Explicit expressions are given for both the surface perturbation pressure and wind components and these are applied in the next section to three simple, but realistic, inversion waveguide models to illustrate the principal features of long nonlinear waves in the atmospheric boundary layer. The main results of the present paper are presented in Section 5. Numerical solutions of the BDO equation are given in Section 5(a) for a wide variety of initial conditions ranging from smooth internal deep-fluid bore waves of infinite extent to long waves of finite volume. One of the most important results to emerge from this investigation is the discovery that relatively benign long wave disturbances in the atmospheric boundary layer can evolve rapidly under ideal uniform waveguide conditions into solitary waves of exceptionally large amplitude. This result has obvious implications for the subject of hazardous aviation wind shear (Christie and Muirhead, 1983, a,b; 1985) and raises a number of interesting questions regarding the role of these disturbances in the initiation and organization of deep convection. The results of a numerical investigation of both the stationary and

time-dependent solutions of the BDO-Burgers equation are given in Section 5(b). Solutions corresponding to deep-fluid time-independent internal bore waves and to decaying spatially localized long wave disturbances are presented in detail and a number of specific models for nonlinear atmospheric waves are proposed, based on these results. Section 6 is devoted to a study of nonlinear wave propagation under conditions where variations in the degree of turbulent friction occur either at a boundary, or as a result of the onset of shear instability in the leading solitary wave components.

2. Properties of Nonlinear Wave Disturbances

The morning glory of the Gulf and Carpentaria provides a particularly good illustration of the properties of long nonlinear wave disturbances in the lower atmosphere. The morning glory appears to originate (Clarke, 1983b; Clarke, 1984; Crook and Miller, 1985; Noonan and Smith, 1986) during the early evening over the central highlands of the Cape York Peninsula in the transformation of a sea-breeze surge from the Coral Sea into an internal long wave disturbance. This disturbance continues to propagate during the following morning towards the south-east over the southern Gulf of Carpentaria on a nocturnal/maritime inversion layer and then inland over the arid interior of northern Australia. The initially smooth long wave disturbance develops undulations along the leading edge which evolve rapidly into discrete solitary waves with amplitudes comparable to the effective depth of the surface-based inversion. Under suitable conditions, the leading solitary wave components produce roll cloud formations which may extend from a base at a few hundred meters to a height of more than two kilometers. These solitary wave roll cloud formations, which typically have a width of about 4 kilometers, seldom produce precipitation; large amplitude disturbances of this type do, however, initiate deep

convection and thunderstorms are frequently observed to develop over the Gulf of Carpentaria in the wake of these disturbances.

The salient features of morning glory wave disturbances may be seen in the selection of surface micropressure records shown in Figures 1 to 3. These records have been chosen to illustrate the principal features of the most commonly observed forms of these disturbances. In many cases, the disturbance appears to have a well-defined horizontal length in the direction of propagation. On occasion, however, these disturbances extend over considerable distances and the form of the disturbance is reminiscent, to some extent, of a classical bore wave on the surface of shallow water. It should be emphasised, however, that an analogy with the classical bore wave phenomenon should not be taken too literally. A careful investigation of the surface pressure signature of morning glory disturbances has shown that the pressure perturbation due to these disturbances is not usually maintained at a constant level over prolonged periods of time which implies that the inversion height does not remain elevated for long periods of time behind the leading edge of these disturbances. The observed decay in surface wind speed behind the leading solitary wave components in these disturbances is also consistent with this interpretation.

On average, most morning glory disturbances have 3 or 4 well-developed solitary wave components. In some cases, these disturbances appear to occur in the form of an essentially asymptotic amplitude-ordered family of solitary waves (see Figure 1) while other morning glory disturbances are observed with only one well-defined solitary wave component along the leading edge (see Figures 2b and 3d) ahead of the main disturbance. In contrast, on occasion, particularly extensive disturbances are observed with 8 or more clearly defined solitary wave components (see Figure 2d). In well-developed disturbances the horizontal separation between the leading solitary wave components is typically between 3 and 10 kilometers and the amplitude of the leading solitary wave is usually within the range from 300 to 1000 meters. Morning glories which originate over the Cape York Peninsula propagate towards the south-west with

speeds between 6 and 18 m/s. Similar nonlinear wave disturbances which originate to the south and south-east are also observed on occasion along the southern margin of the Gulf of Carpentaria (Christie et al., 1981; Smith et al., 1982; Smith et al., 1986).

The extensive aerological observations reported by Clarke et al. (1981), Smith et al. (1982), Clark (1983b), and Smith and Morton (1984) have provided an abundance of data on the environmental waveguide conditions over the southern Gulf of Carpentaria region. Morning glory waves propagate on a stably-stratified boundary-layer inversion underlying an almost neutral elevated layer which extends for several kilometers above the inversion height. The depth of the surface-based inversion is typically between 500 and 1200 meters and the average Brunt-Väisälä period in this waveguide layer is usually in the range from 4 to 6 minutes. The environmental wind component normal to the wavefront is usually towards the disturbance in the inversion layer and along the direction of propagation at higher levels. The ambient normal winds tend to be light at lower levels and are always less than the observed propagation speed of the wave front at higher levels. Smith and Morton (1984) have emphasised that critical levels in the environmental wind structure are apparently absent in the case of morning glory wave disturbances.

3. Evolution Equations for Long Nonlinear Internal Waves in the Atmosphere

The theoretical description of long finite-amplitude internal waves in stratified fluids has received a great deal of attention in recent years. For waves of modest amplitude in shallow homogeneous fluids, the appropriate equation (see, for instance, Benney (1966) and Benjamin (1966)) which describes the time evolution of the vertical displacement at any point in the fluid,

$$\eta(x,z,t) = A(x,t)\varphi(z), \tag{3.1}$$

is the familiar Korteweg-de Vries equation,

$$\frac{\partial A}{\partial t} + c_0\frac{\partial A}{\partial x} + \alpha A\frac{\partial A}{\partial x} + \beta\frac{\partial^3 A}{\partial x^3} = 0. \tag{3.2}$$

Here c_0 is the linear long wave phase speed and the coefficients of the nonlinear and dispersive terms, α and β respectively, along with the vertical modal function, $\varphi(z)$, are determined by the environmental waveguide density profile $\rho_0(z)$ and shear distribution $u_0(z)$. As suggested by Christie et al. (1978), the KdV equation may provide a reasonable first-order model for larger scale atmospheric wave disturbances with horizontal wave lengths comparable to the depth of the troposphere. Here, however, we are concerned primarily with the description of nonlinear wave disturbances which are confined to surface-based inversion waveguides with effective vertical scales of the order of one kilometer. These waves therefore belong to the class of nonlinear wave disturbances in deep fluids first considered by Benjamin (1967) and Davis and Acrivos (1967) and later by Ono (1975). In this case the appropriate scale is determined by the effective depth, h, of the embedded waveguide rather than by the overall effective fluid depth, H. The governing evolution equation for waves of this type is the Benjamin-Davis-Ono equation,

$$\frac{\partial A}{\partial t} + c_0\frac{\partial A}{\partial x} + \alpha A\frac{\partial A}{\partial x} + \delta\frac{\partial^2}{\partial x^2}\mathcal{H}(A) = 0, \tag{3.3}$$

where the linear dispersive term is now given by the Hilbert transform,

$$\mathcal{H}(A(x)) = \frac{1}{\pi}\int_{-\infty}^{\infty}\frac{A(x')}{x'-x}\,dx'.$$

A more general evolution equation for nonlinear waves in a finite-depth fluid, which reduces to the KdV equation in the shallow-fluid limit and to the BDO equation in the infinitely-deep-fluid limit has been given by Joseph (1977) and Kubota et al. (1978).

The Korteweg-de Vries and Benjamin-Davis-Ono evolution equations have been studied extensively and the basic properties of their solutions, especially in the case of

the KdV equation, are now fairly well understood. These equations are known to be completely integrable with infinitely many conservation laws (Miura et al., 1968 (KdV); Nakamura, 1979 (BDO)) and this implies that the solitary wave solutions should exhibit the soliton property; i.e., despite nonlinear interaction, individual solitary waves should emerge unscathed from collision. This is true for the solitary wave solutions of both equations. Indeed, the concept of the soliton originated in a numerical study of the solutions of the Korteweg-de Vries equation (Zabusky and Kruskal, 1965). The N-soliton solution to the KdV equation has been given by Hirota (1971) and the corresponding solution for the BDO equation has been found by Matsuno (1979) and Chen et al. (1979).

The general behaviour of the time-dependent solutions of these basic model equations are similar in many respects. For example, solutions of both equations derived from arbitrary initial data evolve asymptotically into a finite number of amplitude-ordered solitons. Dispersive effects are, however, stronger in deep fluids and the corresponding solutions of these equations differ significantly. In contrast to the KdV equation which describes solitary waves with the familiar exponentially decaying sech^2 profile, the BDO solitons are algebraic. Furthermore, as a property in common with most soliton-generating equations, the KdV equation describes solitary waves which suffer a phase shift on collision. In this regard, the BDO solitons are somewhat exceptional in that they emerge from interaction along their pre-collision trajectories (Case, 1978; Matsuno, 1979). In addition, as emphasised by Koop and Butler (1981), the wavelength-amplitude scaling of BDO solitary waves differs fundamentally from that described by the KdV theory. For waves in unbounded fluids the appropriate wavelength-amplitude relationship is given by

$$\left(\frac{\lambda}{h}\right) = O\left(\frac{a}{h}\right)^{-1} \quad ,$$

while the corresponding scaling requirement for classical shallow-fluid solitary waves is determined by

$$(\frac{\lambda}{H})^2 = O(\frac{a}{H})^{-1} \quad ,$$

where a is the amplitude and λ is a measure of the effective horizontal extent of the wave. Finally it should be noted that the amplitude of solitary waves generated in the decay of arbitrary disturbances in infinitely deep fluids may be substantially larger than the amplitude of KdV solitons created under similar initial conditions in shallow fluids. This important aspect will be examined further in the numerical experiments described below.

Comprehensive treatments of the theory of long internal waves in continuously stratified shear flows have recently been presented by Maslowe and Redekopp (1979, 1980), Tung et al. (1981) and Grimshaw (1981a). Maslowe and Redekopp consider finite-amplitude wave motions in a homogeneous sheared Boussinesq fluid for both bounded and unbounded fluid domains, including the case where upward radiation into a weakly stratified ambient environment is possible. They also examine the possibility of singular modes which may exist in critical layers where the phase speed is equal to the mean flow speed. The theoretical treatment presented by Tung et al. is also concerned with wave propagation in stratified shear flows both with and without critical levels. Their theory is developed for waves in a thin pycnocline embedded in a finite-depth fluid and represents an extension of the theory of Kubota et al. (1978) to parallel shear flows. We shall not consider further the possibility of singular critical layer modes in the interpretation of nonlinear boundary layer atmospheric waves since critical levels have not as yet been identified in the environmental wind structure (Smith and Morton, 1985).

Grimshaw (1981a) has presented a very thorough treatment of long nonlinear internal waves in both shallow and deep fluids, including the influence of slow temporal and spatial variations in the waveguide structure along with the effects of both radiation and frictional damping.

The general theory has also been extended by Grimshaw (1980) to compressible

fluids, including both dry and moist atmospheres. In this treatment, for fluids of infinite extent, the vertical modal function, $\varphi(z)$, satisfies the eigenvalue problem:

$$\frac{\partial}{\partial z}(\rho_o(c_o - u_o)^2 \frac{\partial \varphi}{\partial z}) + \rho_o N^2 \varphi = \nu \frac{\partial}{\partial z}\left[\frac{(c_o-u_o)^2}{c_s^2}\right]\varphi, \tag{3.4a}$$

$$\varphi = 0 \text{ on } z = 0, \tag{3.4b}$$

$$\frac{\partial \varphi}{\partial z} \to 0 \text{ as } z \to \infty, \tag{3.4c}$$

where c_s is the velocity of sound, N is the Brunt-Väisälä frequency defined by $N^2=gd(\ln\theta_v)/dz$ where θ_v is the virtual potential temperature, and the compressibility parameter, ν, is given by $\nu=\gamma g h/c_s^2$ where γ is the ratio of the specific heats and h is the characteristic vertical scale of the inversion waveguide. It will be assumed that the eigenfunctions, $\varphi(z)$, have been normalized to a maximum absolute value of one. This Sturm-Liouville problem generally admits an infinite number of vertical modal functions, each corresponding to a distinct infinitesimal long-wave phase speed, c_o. The lowest mode solution will usually be the only solution of interest since higher modes propagate much slower and are not generally observed in the atmosphere.

It is worth noting that the non-Boussinesq vertical modal equation (3.4a) can be rewritten as a long wavelength form of the Taylor-Goldstein equation for a compressible fluid through the transformation $\bar{\varphi}=(u_o-c_o)\varphi$:

thus,

$$\frac{\partial}{\partial z}(\rho_o \frac{\partial \bar{\varphi}}{\partial z}) + \left[\frac{\rho_o N^2}{(u_o-c_o)^2} - \frac{\frac{\partial}{\partial z}\left[\rho_o \frac{\partial u_o}{\partial z}\right]}{(u_o-c_o)} - \frac{\nu}{(u_o-c_o)^2}\frac{\partial}{\partial z}\left[\frac{(c_o-u_o)^2}{c_s^2}\right]\right]\bar{\varphi} = 0 \tag{3.5}$$

In the Boussinesq approximation, the effect of density variations on the inertial terms may be neglected and for an incompressible fluid equation (3.5) becomes the familiar form of the Taylor-Goldstein equation for zero wavenumber:

$$\frac{\partial^2 \bar{\varphi}}{\partial z^2} + \ell^2(z)\,\bar{\varphi} = 0 \quad , \tag{3.6}$$

where

$$\ell^2(z) = \frac{N^2}{(u_o - c_o)^2} - \frac{\dfrac{\partial^2 u_o}{\partial z^2}}{(u_o - c_o)}$$

is the Scorer parameter (Scorer, 1949). Clarke (1983b) and Noonan and Smith (1985) have examined the relative importance of the stratification and wind profile curvature terms in the Scorer parameter for pre-morning glory environments. The wind curvature term tends to dominate above 200 meters and Clarke suggests, on the basis of an average over eight individual events, that both contributions might be viewed together as an "effective stratification", linearly decreasing with height. A very thorough discussion of the relative importance of the wind curvature term in the Scorer parameter under conditions where strongly trapped nonlinear wave propagation is possible has recently been given by Crook (1986).

Following Grimshaw (1980), for a homogeneous compressible fluid, the coefficients α and δ in the BDO equation are given by

$$\alpha = \frac{1}{I} \int_o^\infty \left\{ 3\rho_o (c_o - u_o)^2 \left(\frac{\partial \varphi}{\partial z}\right)^3 - \frac{7}{2} \nu \rho_o \frac{N^2 \varphi^3}{c_s^2} \right\} dz, \tag{3.7a}$$

$$\delta = \frac{1}{I} \left\{ \rho_o (c_o - u_o)^2 \varphi^2 \right\}_{z \to \infty} , \tag{3.7b}$$

where

$$I = 2 \int_o^\infty \left\{ \rho_o (c_o - u_o) \left(\frac{\partial \varphi}{\partial z}\right)^2 + \nu \rho_o \varphi^2 \frac{\partial}{\partial z} \left[\frac{c_o - u_o}{c_s^2} \right] \right\} dz \tag{3.7c}$$

In most cases, as noted by Grimshaw (1980), the effects due to compressibility are small and the lower atmosphere may be taken to be incompressible provided the appropriate Brunt-Väisälä frequency for a dry or moist atmosphere is used in the equations.

The evolution of the streamline pattern within a stably stratified atmospheric inversion waveguide may be calculated from the vertical displacement given by (3.1). Above this region the amplitude of the disturbance in the neutrally stratified fluid decays algebraically and the vertical displacement may be obtained, as described by Benjamin (1967), using Fourier transforms:

$$\eta(x,z,t) = \int_{-\infty}^{\infty} \mathcal{F}(A)\exp[-ikx-|k|(z-h)]dk, \tag{3.8a}$$

where

$$\mathcal{F}(A) = \frac{1}{2\pi} \int_{-\infty}^{\infty} A(x,t)\exp(ikx)dx \tag{3.8b}$$

Long nonlinear waves in the atmospheric boundary layer are often detected using an array of microbarometers. By applying Bernoulli's equation to the surface streamline it is easily shown that the surface perturbation pressure associated with the passage of a nonlinear wave disturbance is given by

$$\Delta P(x,t) = \Delta P_{hs}(x,t) + \Delta P_{hd}(x,t), \tag{3.9a}$$

where

$$\Delta P_{hs}(x,t) = gA(x,t)\left[\int_0^h \rho(z)\left(\frac{\partial \varphi}{\partial z}\right)\, dz - \rho_2\right] , \tag{3.9b}$$

with

$$\rho(z) = \rho_o(z), \quad z < h,$$
$$\rho(z) = \rho_2 \quad , \quad z > h,$$

and

$$\Delta P_{hd}(x,t) = \frac{1}{2}\rho_o(0)(u_o(0) - c)^2 \left[1 - \frac{1}{\left[1+A(x,t)\frac{\partial \varphi(0)}{\partial z}\right]^2}\right] . \tag{3.9c}$$

In most cases of interest, the hydrostatic term, ΔP_{hs}, is significantly larger than the hydrodynamic term, ΔP_{hd}, and the inclusion of this term in the expression for the surface perturbation pressure appears to account for the discrepancy found by Noonan and Smith (1985) in their study of morning glory solitary waves. A vertical

acceleration term could also be included in (3.9a). The results of a simple calculation show however that vertical accelerations associated with nonlinear wave motions in a boundary layer waveguide contribute only a negligible correction to the surface perturbation pressure.

The horizontal and vertical wind components in the stratified inversion layer are given, respectively, by

$$u^i(x,z,t) = \frac{u_o(z)+cA(x,t)\frac{\partial\varphi(z)}{\partial z}}{1 + A(x,t)\frac{\partial\varphi(z)}{\partial z}} , \tag{3.10a}$$

and

$$w^i(x,z,t) = - \frac{(c - u_o(z))\frac{\partial A(x,t)}{\partial x}\varphi(z)}{1 + A(x,t)\frac{\partial\varphi(z)}{\partial z}} . \tag{3.10b}$$

In the outer neutrally stratified region above the inversion waveguide the wind components may be determined by evaluating

$$u^0(x,z,t) = \frac{u_o(z) + cI_1}{1 + I_1} , \tag{3.11a}$$

$$w^0(x,z,t) = - \frac{(c - u_o(z))I_2}{1 + I_1} , \tag{3.11b}$$

where

$$I_1 = -\int_{-\infty}^{\infty} |k| \exp[-ikx - |k|(z-h)] \, \mathcal{F}(A)dk, \tag{3.11c}$$

and

$$I_2 = - \int_{-\infty}^{\infty} ik \exp[-ikx - |k|(z-h)] \, \mathcal{F}(A)dk. \tag{3.11d}$$

The Benjamin-Davis-Ono equation has time-independent solutions, A=f(x-ct), in the form of algebraic solitary waves:

$$A(x,t) = \frac{a\lambda^2}{(x-ct)^2 + \lambda^2} , \tag{3.12a}$$

$$c - c_o = \frac{1}{4}\alpha a = \frac{\delta}{\lambda} . \tag{3.12b}$$

For stationary waves of this type, expressions for the vertical displacement+ and wind components in the upper neutrally stratified region may be determined explicitly from (3.8) and (3.11) as

$$\eta(x,z,t) = \frac{a\lambda(\lambda + z - h)}{(x - ct)^2 + (\lambda + z - h)^2} , \tag{3.13}$$

$$u^0(x,z,t) = K^{-1}\left[\frac{u_o(z) + ca\lambda\{(x - ct)^2 - (\lambda + z - h)^2\}}{\{(x - ct)^2 + (\lambda + z - h)^2\}^2}\right] , \tag{3.14a}$$

and

$$w^0(x,z,t) = K^{-1}\left[\frac{4a\lambda(c - u_o(z))(\lambda + z - h)(x - ct)}{\{(x - ct)^2 + (\lambda + z - h)^2\}^2}\right] , \tag{3.14b}$$

where

$$K = 1 + \frac{a\lambda\{(x - ct)^2 - (\lambda + z - h)^2\}}{\{(x - ct)^2 + (\lambda + z - h)^2\}^2} .$$

The Benjamin-Davis-Ono equation also has periodic long wave stationary solutions (Benjamin, 1967) in the form of an infinite train of supercritical constant amplitude waves which represent the deep-fluid counterpart to the well known elliptic cosine or 'cnoidal' wave solutions of the classical Korteweg-de Vries equation. It should be emphasised that long nonlinear guided wave disturbances in the lower atmosphere seldom, if ever, occur in the form of a long sequence of periodic constant amplitude waves. This is as expected since 'cnoidal' waves cannot be generated in the evolution

---

Footnote+ The expression for the outer solitary wave solution given in (3.13) agrees with the dimensionless expression in Davis and Acrivos (1967) and, after correction for a misprint, with equation (3.83) in Benjamin (1967).

of any realistic physical disturbance of limited spatial extent. These stationary periodic wave solutions will therefore not be considered further as a possible model for nonlinear boundary layer waves. In contrast, the solitary wave components play a fundamentally important role in the description of the evolution of long wave disturbances of this type.

Up to this point this discussion has been primarily concerned with the description of waves of modest amplitude in a homogeneous waveguide embedded in a neutrally stratified fluid of infinite extent. It can be anticipated that this relatively simple model will provide a first-order description of nonlinear boundary layer waves as they propagate under ideal conditions over level terrain for distances of the order of perhaps a few hundred kilometers. A horizontally homogeneous waveguide model may however represent an over-simplification of lower atmospheric structure. It must also be expected that frictional damping will play an important role in the evolution of these disturbances. In addition, a perturbation term which accounts for energy loss through radiation into the upper atmosphere may also be required under some conditions. All of these factors have been included in the thorough analysis presented by Grimshaw (1981a; 1982) who shows that the appropriate evolution equation for nonlinear waves in a viscid, inhomogeneous, sheared waveguide subject to radiation damping is given by a generalization of the BDO equation:

$$\frac{\partial A}{\partial t} + c_o\frac{\partial A}{\partial x} + \alpha(x,t)A\frac{\partial A}{\partial x} + \delta(x,t)\mathcal{B}\left(\frac{\partial A}{\partial x}\right) - \mu_m(x,t)\mathcal{V}_m(A) = 0, \qquad (3.15a)$$

where

$$\mathcal{B}(A) = \frac{-1}{2\pi}\int_{-\infty}^{\infty}\left[\tau^2 - \frac{N_\infty^2}{c_o^2}\right]^{\frac{1}{2}} \exp(i\tau x)\,\mathcal{F}(A)d\tau\ , \qquad (3.15b)$$

N_∞ is the Brunt-Väisälä frequency in the weakly stratified fluid above the waveguide and $\mathcal{V}_m(A)$ is a pseudo-differential operator which describes frictional dissipation:

$$\mathcal{V}_m(A) = \frac{1}{2\pi} \int_{-\infty}^{\infty} (-ik)^m \exp(ikx)\, \mathcal{F}(A)dk, \qquad (3.15c)$$

$0 < m < 3;\ m \neq 1.$

In this equation, the coefficients α, δ and μ are slowly varying functions which reflect the temporal and spatial variations in the waveguide structure. Even when α and δ are constant and frictional dissipative processes are negligible, energy is continually radiated away due to the excitation and outward propagation of internal waves in the ambient upper fluid. This equation therefore does not possess steady finite-volume travelling wave solutions. The detailed theory of the evolution of a solitary wave in an inhomogeneous waveguide subject to both radiation and frictional damping has been given by Grimshaw (1981a,b,c; 1982). The influence of radiation damping on the solitary wave solution has also been treated analytically in the adiabatic approximation by Maslowe and Redekopp (1981) and numerically by Pereira and Redekopp (1980). It should be noted that the available observational evidence (Clarke et al., 1981; Clark, 1983b; Smith and Morton, 1984; see also the discussion in Crook, 1986), while by no means definitive, suggests that radiation damping may not be a significant factor in the evolution of most nonlinear boundary layer wave disturbances. The influence of energy radiation into the upper atmosphere on the evolution of long nonlinear wave disturbances will not be considered further in this paper. In contrast, frictional damping is likely to be important under most boundary layer conditions. We shall therefore focus our attention in this initial study on a detailed investigation of finite-amplitude long wave propagation in a horizontally homogenous inversion waveguide under both ideal conditions where dissipative processes may be neglected and under conditions where turbulent frictional damping has a significant influence on the evolution pattern. As will be seen, the results of this investigation provide a fairly satisfactory description of the principle features of long wave disturbances in the lower atmosphere.

The linear operator $\mathcal{V}_m$ in equation (3.15) provides a general description of both laminar boundary layer friction ($m = \frac{1}{2}$) and turbulent bottom friction ($m = 2$) where the shear stress is specified by a Chezy law. We shall consider only the influence of a turbulent boundary layer as laminar frictional dissipation in unlikely to be of any significance to the study of long waves in the atmosphere. In this case, a Burgers diffusion term results and we shall refer to the resulting perturbed evolution equation,

$$\frac{\partial A}{\partial t} + c_o \frac{\partial A}{\partial x} + \alpha A \frac{\partial A}{\partial x} + \delta \frac{\partial^2}{\partial x^2} \mathcal{H}(A) - \mu \frac{\partial^2 A}{\partial x^2} = 0 \quad , \tag{3.16}$$

as the Benjamin-Davis-Ono-Burgers equation. Since a general analytical solution to (3.16) has not been found, the time evolution of arbitrary long wave disturbances as governed by (3.16) will be determined numerically.

Equation 3.15 may be regarded as a fairly realistic model equation for the description of nonlinear atmospheric waves of modest amplitude under uniform waveguide conditions. The observed properties of morning glory waves suggest that they are essentially a one-dimensional disturbance. Under some conditions, however, such as when transverse variations in waveguide structure occur, the description of these disturbances may require an extension of the BDO theory to two spatial dimensions (see, e.g., Ablowitz and Segur, 1980; Redekopp, 1980). Furthermore, a theoretical treatment which includes the effects of the Earth's rotation (Grimshaw, 1985) may be required in some instances, especially at higher latitudes when nonlinear wave disturbances are subject to the influence of a topographic boundary.

4. Inversion Waveguide Models

Before proceeding to the results of a numerical study of the evolution equations it is worth considering solutions to the vertical modal eigenvalue problem (3.4) corresponding to three surface-based inversion waveguide models as an illustration of

the principal features of finite amplitude wave motions in the lower atmosphere. General solutions to (3.4) for arbitrary shear and stratification are not known and for many cases of interest this system must be treated numerically (Noonan and Smith, 1985). Under some conditions, however, the inversion waveguide can be approximated by a simple model and useful analytical solutions corresponding to realistic density and shear profiles can be found. Since our interest here is focussed primarily on the time evolution problem we shall consider only the following simple analytical models for deep-fluid nonlinear wave propagation in an incompressible, horizontally homogeneous boundary layer inversion with shear.

Model a. Two fluids of constant density with linear wind profile

This is perhaps the simplest possible boundary layer waveguide model with shear. In this case we shall suppose that the upper and lower fluids have constant densities ρ_2 and ρ_1 respectively. The ambient wind component along the direction of wave propagation is assumed to be constant ($u_0(z)=u_\infty$) in the upper layer and linear ($u_0(z)=u_1+u_2 z$) in the lower layer. The unperturbed interface lies at a height h. It is easily seen that the general solution to the linear eigenvalue equation (3.4) within the inversion layer,

$$\frac{\partial}{\partial z}\left[(c_0 - u_0(z))^2 \frac{\partial \varphi}{\partial z}\right] = 0,$$

which satisfies the dynamic boundary condition,

$$\varphi'(h) = \frac{g(\rho_1(h) - \rho_2(h))}{\rho_1(h)\,(c_0 - u_0(h))^2}\ , \qquad (4.1)$$

at the interface z = h (continuity of pressure, cf. Benjamin, 1966) is given by

$$\varphi(z) = \frac{g(\rho_1 - \rho_2)}{\rho_1} \int \frac{dz}{(c_0 - u_0(z))^2} + B \quad , \tag{4.2}$$

where c_0 and B are determined by the lower boundary conditon, $\varphi(0) = 0$, and the normalization condition, $\varphi(h) = 1$. Thus, when $u_0(z)$ is linear, the solution in the lower layer is given by

$$\varphi(z) = \frac{(c_0 - u_1 - u_2 h)}{(c_0 - u_1 - u_2 z)} \frac{z}{h} \quad , \tag{4.3}$$

$$\text{with} \quad c_0 = u_1 + \frac{u_2 h}{2} \pm \frac{1}{2} \left[(u_2 h)^2 + \frac{4gh(\rho_1 - \rho_2)}{\rho_1} \right]^{\frac{1}{2}} \tag{4.4}$$

The coefficients α and δ in the evolution equation (3.3) can be evaluated directly from (3.7) as

$$\alpha = \frac{3(c_0 - u_1)^2 - 3(c_0 - u_1)u_2 h + u_2^2 h^2}{h(2(c_0 - u_1) - u_2 h)} \quad , \tag{4.5}$$

$$\text{and} \quad \delta = \frac{h\rho_2 (c_0 - u_\infty)^2}{\rho_1 (2(c_0 - u_1) - u_2 h)} \quad . \tag{4.6}$$

For this particularly simple flow model the horizontal and vertical wind components in the inversion layer (3.10) are given by

$$u^i(x,z,t) = \frac{h(u_1 + u_2 z)(c_0 - u_1 - u_2 z)^2 + cA(x,t)(c_0 - u_1 - u_2 h)(c_0 - u_1)}{h(c_0 - u_1 - u_2 z)^2 + A(x,t)(c_0 - u_1 - u_2 h)(c_0 - u_1)} \quad , \tag{4.7}$$

$$w^i(x,z,t) = \frac{(u_1 + u_2 z - c)(c_0 - u_1 - u_2 h)(c_0 - u_1 - u_2 z) z \frac{\partial A(x,t)}{\partial x}}{h(c_0 - u_1 - u_2 z)^2 + A(x,t)(c_0 - u_1 - u_2 h)(c_0 - u_1)} \quad , \tag{4.8}$$

and the surface perturbation pressure as determined by formula (3.9) is

$$\Delta P(x,t) = (\rho_1 - \rho_2) g A(x,t)$$

$$+ \tfrac{1}{2}\rho_1 (u_1 - c)^2 \left\{ 1 - \frac{(c_0 - u_1)^2 h^2}{(h(c_0 - u_1) + (c_0 - u_1 - u_2 h)A(x,t))^2} \right\} \quad . \tag{4.9}$$

This waveguide model must be regarded as an over-simplification of the properties of the atmospheric boundary layer. It does, however, provide a reasonable first-order approximation for the description of nonlinear atmospheric waves in a surface-based inversion with shear and can be used to illustrate the basic features of these disturbances.

Model b. Constant N, linear wind profile in lower layer; density jump at interface.

We shall now turn our attention to a more realistic waveguide model in which a layer of depth h, with constant Brunt-Väisälä frequency, N_1, and linear wind profile, $u_0(z) = u_1 + u_2 z$, lies beneath a neutrally stable layer ($N = 0$) with constant wind component, u_∞. We shall suppose as well that a density discontinuity, $\Delta\rho = \rho_1(h) - \rho_2(h)$, exists across the interface $z = h$. The solution to the eigenvalue problem for this model in the absence of shear with $\Delta\rho = 0$ has been described by Benjamin (1967) for both Boussinesq and non-Boussinesq fluids and also by Grimshaw (1981) as an illustration of the properties of second-order deep-fluid solitary waves. Solutions for this flow configuration when shear is present but with $\Delta\rho = 0$ have also been found by Maslowe and Redekopp (1979, 1980) and Clarke et al. (1981). We extend these results here to include the influence of a potential temperature discontinuity at the interface between the lower shear layer and the upper neutrally stratified layer. In addition, explicit expressions are obtained for the coefficients in the evolution equation, the wind components in the inversion layer and the surface perturbation pressure.

We first consider a direct extension of the non-Boussinesq results of Benjamin (1967) to a flow model with $N = N_1$ in the lower layer, constant wind components, u_1 and u_∞, in the lower and upper layers respectively, and with a density jump, $\Delta\rho = \rho_1(h) - \rho_2$ at the interface $z = h$. In this case, since $\rho_1(z) = \rho_S \exp(-N_1^2 z/g)$, the

linear eigenvalue equation below the interface is given by

$$\frac{\partial^2\varphi}{\partial z^2} - \frac{N_1^2}{g}\frac{\partial\varphi}{\partial z} + \frac{N_1^2}{(c_o-u_1)^2}\varphi = 0 \quad . \tag{4.10}$$

The normalized solution of (4.10) which satisfies both the kinematic boundary condition, $\varphi(0)=0$, and the dynamic boundary condition (4.1) is given by

$$\varphi(z) = e^{\frac{N_1^2(z-h)}{2g}}\frac{\sin qz}{\sin qh} \quad , \tag{4.11}$$

where

$$q^2 = \frac{N_1^2}{(c_o-u_1)^2} - \left[\frac{N_1}{2g}\right]^2 \quad , \tag{4.12}$$

and the eigenvalues, c_o, are determined by the solution of

$$\frac{q}{\tan(qh)} + \frac{N_1^2}{2g} = \frac{K}{(c_o-u_1)^2} \quad , \tag{4.13}$$

where

$$K = \frac{g(\rho_1(h)-\rho_2(h)}{\rho_1(h)} \approx \frac{g\Delta\theta}{\theta} \quad ,$$

with θ the potential temperature and $\Delta\theta$ the potential temperature discontinuity at the top of the stratified inversion layer. Since $N_1^2h/g \ll 1$, the solution in the Boussinesq approximation for a flow configuration with constant wind components is given by

$$\varphi(z) = \frac{\sin\left[\frac{N_1 z}{c_o-u_1}\right]}{\sin\left[\frac{N_1 h}{c_o-u_1}\right]} \tag{4.14}$$

with the eigenvalue condition

$$\frac{N_1 h}{(c_o-u_1)} = \tan^{-1}\left[\frac{(c_o-u_1)N_1}{K}\right] + n\pi, \quad n=0,\pm1,\pm2\ldots \tag{4.15}$$

where n is the mode number.

We now present the solution of the eigenvalue problem for the more general flow model with a linear wind profile in the stratified lower layer and a capping inversion at z=h. The solution for this configuration is most readily achieved by treating the problem in the Boussinesq approximation and solving the resulting Taylor-Goldstein equation (3.6). In this case the eigenvalue problem for $\bar{\varphi} = (u_0(z)-c_0)\varphi$ is given by

$$\frac{\partial^2\bar{\varphi}}{\partial z^2} + \frac{J\, u_2^2}{(c_0-u_1-u_2z)^2}\,\bar{\varphi} = 0 \quad , \tag{4.16a}$$

with

$$\bar{\varphi}(0) = 0 \quad , \tag{4.16b}$$

$$\bar{\varphi}(h) = u_0(h)-c_0 = u_1+u_2h-c_0, \tag{4.16c}$$

and

$$\bar{\varphi}'(h) = u_0'(h) + \frac{K}{(u_0(h)-c_0)} \quad , \tag{4.16d}$$

where $J = N_1^2/u_2^2$ is the Richardson number for the inversion layer. The normalized solution for φ which satisfies the surface boundary condition is

$$\varphi(z) = \frac{|c_0-u_1-u_2h|^{\frac{1}{2}}\sin\left[\sigma\ln\left|\frac{c_0-u_1-u_2z}{c_0-u_1}\right|\right]}{|c_0-u_1-u_2z|^{\frac{1}{2}}\sin\left[\sigma\ln\left|\frac{c_0-u_1-u_2h}{c_0-u_1}\right|\right]} \quad , \tag{4.17}$$

where $\sigma = (J-\frac{1}{4})^{\frac{1}{2}}$. It will be assumed that σ is real and thus the ambient stratified shear flow is linearly stable. Substitution of the solution for $\varphi(z)$ into (4.16d) yields the eigenvalue condition

$$c_0 = u_1 + \frac{u_2h}{1 - e^{\kappa}} \quad , \tag{4.18}$$

with

$$\kappa = \frac{1}{\sigma}\tan^{-1}\left[\frac{2\sigma}{1 - \frac{2K}{u_2(c_o-u_1-u_2h)}}\right] - \frac{n\pi}{\sigma} \quad , \; n=0,\pm1,\pm2,\ldots$$

The coefficients appearing in the BDO equation can now be evaluated from the formulae given in (3.7). After a lengthy, but straight-forward computation, we find

$$\alpha = \frac{2Ju_2\sin\xi\{|c_o-u_1|^{3/2}J^{\frac{1}{2}}S + |c_o-u_1-u_2h|^{3/2}\}}{(2+J)|c_o-u_1|^{\frac{1}{2}}\sigma\{|c_o-u_1|(1-R)-|c_o-u_1-u_2h|\}} \tag{4.19}$$

and

$$\delta = \frac{|c_o-u_1|(u_\infty-c_o)^2\sin^2\xi}{(J-\frac{1}{4})u_2\{|c_o-u_1|(1-R) - |c_o-u_1-u_2h|\}} \quad , \tag{4.20}$$

where

$$R = \frac{2K^2\sin^2\xi}{(J-\frac{1}{4})u_2^2(c_o-u_1-u_2h)^2(2\sigma\cot\xi - 1)} \quad ,$$

$$S = \frac{K\sin\xi}{u_2(c_o-u_1-u_2h)\sigma J^{\frac{1}{2}}}\left[1 - \frac{[(2+J)K^2\sin^2\xi+2u_2^2(c_o-u_1-u_2h)^2\sigma^2J]}{u_2^2(c_o-u_1-u_2h)^2(2\sigma\cot\xi - 1)\sigma^2}\right] \quad ,$$

and

$$\xi = \sigma\ln\left|\frac{c_o-u_1-u_2h}{c_o-u_1}\right| \quad .$$

Explicit expressions for the wind components in the shear layer as described by this fairly realistic waveguide model can also be obtained. The substitution of (4.17) into (3.10) gives

$$u^i(x,z,t) = \frac{(u_1+u_2z)|r-z|^{3/2}\sin\xi + cA(x,t)\mathrm{sgn}(z-r)|r-h|^{\frac{1}{2}}J^{\frac{1}{2}}\sin\chi(z)}{|r-z|^{3/2}\sin\xi + A(x,t)\mathrm{sgn}(z-r)|r-h|^{\frac{1}{2}}J^{\frac{1}{2}}\sin\chi(z)} \tag{4.21}$$

and

$$w^i(x,z,t) = \frac{(u_1+u_2z-c)\frac{\partial A(x,t)}{\partial x}\sin\left[\sigma\ln\left|\frac{r-z}{r}\right|\right]|r-h|^{\frac{1}{2}}|r-z|}{|r-z|^{3/2}\sin\xi + A(x,t)\mathrm{sgn}(z-r)|r-h|^{\frac{1}{2}}J^{\frac{1}{2}}\sin\chi(z)} \quad , \tag{4.22}$$

where $r = (c_o - u_1)/u_2$,

and $\chi(z) = -\sigma \ln\left|\frac{r - z}{r}\right| + \tan^{-1}(2\sigma)$.

Since $N_1^2 h/g \ll 1$, we shall approximate the density distribution in the inversion layer by $\rho(z) = \rho_s(1 - N_1^2 z/g)$. Equation (3.9) can then be evaluated to give the surface perturbation pressure,

$$\Delta P(x,t) = gA(x,t)\left[\rho_s + \frac{\rho_s N_1^2 r\sigma}{gJ^{\frac{1}{2}}}\left\{G\left[F + \left|\frac{r - h}{r}\right|\left(\frac{1}{\sigma} - F\right)\right]\right.\right.$$

$$\left.\left. - \frac{1}{\sigma}\left|\frac{r - h}{r}\right|^{\frac{1}{2}} \frac{\sin\chi(0)}{\sin\xi}\right\} - \rho_2\right]$$

$$+ \tfrac{1}{2}\rho_s(u_1 - c)^2 \left[1 - \frac{|r|^3 \sin^2\xi}{(|r|^{3/2}\sin\xi - A(x,t)\mathrm{sgn}(r)J^{\frac{1}{2}}\sin\chi(0)|r-h|^{\frac{1}{2}})^2}\right] , \quad (4.23)$$

with $F = \dfrac{4J}{2\sigma(1 - 2\sigma\cot\xi)}$,

and $G = \dfrac{K}{N_1(u_1 + u_2 h - c_o)}$.

If we now take the limit of the above results as $u_2 \to 0$ we obtain the evolution equation coefficients, the waveguide wind components and surface perturbation pressure for a flow model with a capping inversion above a bottom layer with constant Brunt-Väisälä frequency and constant ambiant winds. Thus, φ and c_o are defined for this simplified model by (4.14) and (4.15) respectively and expressions (4.19) to (4.23) reduce, when $u_2 = 0$, to

$$\alpha = \frac{2N_1\left\{3 - \sin^2\left[\dfrac{N_1 h}{c_o - u_1}\right]\right\}}{\dfrac{2N_1 h}{(c_o - u_1)} + \sin\left[\dfrac{2N_1 h}{c_o - u_1}\right]} , \quad (4.24)$$

$$\delta = \frac{\dfrac{2(u_\infty - c_o)^2}{N_1}\sin^2\left[\dfrac{N_1 h}{c_o - u_1}\right]}{\dfrac{2N_1 h}{(c_o - u_1)} + \sin\left[\dfrac{2N_1 h}{c_o - u_1}\right]} , \tag{4.25}$$

$$u^i(x,z,t) = \frac{u_1 \sin\left[\dfrac{N_1 h}{c_o - u_1}\right] + \dfrac{cA(x,t)N_1}{(c_o - u_1)}\cos\left[\dfrac{N_1 z}{c_o - u_1}\right]}{\sin\left[\dfrac{N_1 h}{c_o - u_1}\right] + \dfrac{A(x,t)N_1}{(c_o - u_1)}\cos\left[\dfrac{N_1 z}{c_o - u_1}\right]} , \tag{4.26}$$

$$w^i(x,z,t) = \frac{(u_1 - c)\dfrac{\partial A(x,t)}{\partial x}\sin\left[\dfrac{N_1 z}{c_o - u_1}\right]}{\sin\left[\dfrac{N_1 h}{c_o - u_1}\right] + \dfrac{A(x,t)N_1}{(c_o - u_1)}\cos\left[\dfrac{N_1 z}{c_o - u_1}\right]} , \tag{4.27}$$

and

$$\Delta P(x,t) = \frac{N_1 \rho_s A(x,t)(c_o - u_1)}{\sin\left[\dfrac{N_1 h}{c_o - u_1}\right]} + \tfrac{1}{2}\rho_s (u_1 - c)^2 \left\{ 1 - \frac{\sin^2\left[\dfrac{N_1 h}{c_o - u_1}\right]}{\left[\sin\left[\dfrac{N_1 h}{c_o - u_1}\right] + \dfrac{A(x,t)N_1}{(c_o - u_1)}\right]^2} \right\} . \tag{4.28}$$

Finally, if we also let $\Delta\rho \to 0$ in the eigenvalue condition (4.15) we find the solution for the simplest form of this waveguide model corresponding to a flow configuration with constant Brunt-Väisälä frequency in the surface-based inversion layer and constant winds. In this case

$$\varphi(z) = (-1)^{n+1}\sin\left[\frac{2n-1}{2h}\pi z\right], \quad n=1,2,3\ldots, \tag{4.30}$$

$$c_o = u_1 \pm \frac{N_1 h}{(n-\frac{1}{2})\pi} , \tag{4.31}$$

and the coefficients in the BDO equation are

$$\alpha = \frac{2(c_o - u_1)}{h} , \tag{4.32}$$

and

$$\delta = \frac{4h}{[(2n-1)\pi]^2}\frac{(c_o - u_\infty)^2}{(c_o - u_1)} . \tag{4.33}$$

The substitution of (4.30) into the formulae for the inversion waveguide wind compoents (3.10) and surface perturbation pressure (3.9) leads immediately to

$$u^i(x,z,t) = \frac{(-1)^{n+1}u_1 + \frac{cA(x,t)(2n-1)\pi}{2h}\cos\left[\frac{(2n-1)\pi z}{2h}\right]}{(-1)^{n+1} + \frac{A(x,t)(2n-1)\pi}{2h}\cos\left[\frac{(2n-1)\pi z}{2h}\right]} \tag{4.34}$$

$$w^i(x,z,t) = \frac{(u_1 - c)\sin\left[\frac{(2n-1)\pi z}{2h}\right]\frac{\partial A(x,t)}{\partial x}}{(-1)^{n+1} + \frac{A(x,t)(2n-1)\pi}{2h}\cos\left[\frac{(2n-1)\pi z}{2h}\right]} \tag{4.35}$$

and

$$\Delta P(x,t) = (-1)^{n+1}\frac{2hA(x,t)\rho_S N_1^2}{(2n-1)\pi} + \tfrac{1}{2}\rho_S(u_1-c)^2\left\{1 - \frac{4h^2}{\left[(-1)^{n+1}+A(x,t)(2n-1)\pi\right]^2}\right\}. \tag{4.36}$$

Model c. Sech^2 profile for N^2 with constant fluid velocities

As a final illustration of boundary-layer inversion waveguide models for which a solution in closed form can be obtained we consider a model in which the Brunt-Väisälä frequency in the lower layer is given by $N^2=N_0^2\mathrm{sech}^2(z/h)$ and a very simple shear structure is adopted with constant velocity components, u_2 and u_∞, in the upper neutrally stable (N=0) and lower density-stratified fluids respectively. It should be noted that in this case the boundary between the lower stably stratified layer and the upper homogeneous layer is not precisely defined. It is clear, however, that the properties of the solution will be practically independent of the exact position of the boundary provided N^2 at the boundary is $<<N_0^2$. We shall assume that the wind component, u_1, in the lower layer extends from the surface to a height where N^2 effectively vanishes and further contributions to the integrals for α and δ (3.7a,b) are negligible. It should be emphasized that in this case h is the <u>effective depth</u> of the lower fluid and it is this effective depth which determines the scale by which displacement amplitudes and wavelengths are measured. Again, the Boussinesq approximation will be used in the treatment of this model. This model is a direct extension of Benjamin's theory (Benjamin, 1967) for antisymmetric wave modes in a

pycnocline embedded in a unbounded fluid. As discussed by Benjamin, the space above the plane of symmetry, z=0, is dynamically similar, in the Boussinesq approximation, to the space below and a model for first mode waves in a boundary layer waveguide can be obtained by simply introducing a rigid surface at z=0. This model has also been considered by Grimshaw (1981) when u_0=0 as an illustration of the properties of second-order deep fluid solitary waves. It follows readily that the solution for the lowest mode when the two fluids have constant velocity components is given by

$$\varphi(z) = \tanh(z/h), \tag{4.37}$$

$$\alpha = \frac{6}{5h}(c_o - u_1), \tag{4.38}$$

$$\delta = \frac{3h}{4}\frac{(c_o - u_\infty)^2}{(c_o - u_1)}, \text{ and} \tag{4.39}$$

$$c_o = u_1 \pm \frac{N_o h}{\sqrt{2}}. \tag{4.40}$$

The expressions for the horizontal and vertical wind components in the lower stratified layer may be determined directly from (3.10) as

$$u^i(x,z,t) = \frac{u_1 h + cA(x,t)\mathrm{sech}^2(z/h)}{h + A(x,t)\mathrm{sech}^2(z/h)}, \tag{4.41}$$

and

$$w^i(x,z,t) = \frac{h(u_1 - c)\tanh(z/h)\frac{\partial A(x,t)}{\partial x}}{h + A(x,t)\mathrm{sech}^2(z/h)}. \tag{4.42}$$

In this example, the upper limit of integration in (3.9b) may be taken as ∞ and for $N_0^2 h/g \ll 1$ the hydrostatic component of the surface perturbation pressure is given to a good approximation by

$$\Delta P_{hs}(x,t) = gA(x,t)\rho_s \left[\int_0^\infty \left[1 - \frac{N_o^2 h}{g}\right]\tanh(z)\,\mathrm{sech}^2(z)\,dz - \left[1 - \frac{N_o^2 h}{g}\right]\right]$$

$$= \tfrac{1}{2}h\rho_s A(x,t)N_o^2 \quad . \tag{4.43}$$

Thus, the total surface perturbation pressure corresponding to the first mode in this model is given by

$$\Delta P(x,t) = \tfrac{1}{2}h\rho_s A(x,t)N_o^2 + \tfrac{1}{2}\rho_s (u_1 - c)^2\left[1 - \frac{h^2}{(h+A(x,t))^2}\right] \quad . \tag{4.44}$$

The inversion waveguide models discussed in this section have been chosen to illustrate the properties of nonlinear atmospheric waves because they correspond to reasonably realistic boundary layer flow conditions and because they admit analytical solutions in closed form. As an illustration of the principal features of long nonlinear waves, we present in Figures 4 and 5 the relative streamline patterns, surface perturbation pressures, and wind fields for both a solitary wave and an essentially asymptotic amplitude-ordered family of solitary waves propagating as disturbances in the lowest mode (n=1) in typical surface-based inversion waveguides as described by the simplest form of Model b with $\Delta\rho=u_0=0$ and constant Brunt-Väisälä frequency in the inversion layer.

5. Numerical Solutions

In this section we shall consider a number of models for the evolution of nonlinear atmospheric waves which are based on either the inviscid Benjamin-Davis-Ono equation (3.3) or on the Benjamin-Davis-Ono-Burgers equation (3.16) with turbulent frictional damping. In this initial study we shall suppose that the environmental waveguide is horizontally homogeneous; i.e., the ambient density, ρ_0, and wind component, u_0, along the direction of propagation are both functions of height only and thus the coefficients α and δ in the evolution equation are constant. We shall, however, in some of the numerical experiments (see Section 6) examine the effect of a temporally and spatially varying frictional term .

It will be convenient to study the solutions of the BDO-Burgers equation in a coordinate system which moves with the linear phase speed c_0. The evolution equation may then be rewritten in terms of non-dimensional variables as

$$\frac{\partial U}{\partial T} + U\frac{\partial U}{\partial X} + \mathcal{H}\left[\frac{\partial^2 U}{\partial X^2}\right] - \epsilon\frac{\partial^2 U}{\partial X^2} = 0 \quad , \tag{5.1a}$$

where

$$X = \frac{1}{h}(x - c_0 t), \tag{5.1b}$$

$$T = \frac{\delta}{h^2}t \ , \tag{5.1c}$$

$$U(X,T) = \frac{\alpha h}{\zeta}A(x,t), \tag{5.1d}$$

and ϵ is related to the eddy diffusivity coefficient, μ, by $\epsilon = \mu/\delta$.

The accuracy of the numerical solutions described below has been checked by comparing the theoretical and numerical values of the lower order conserved polynominal invariants. The first three conservation laws of the Benjamin-Davis-Ono equation (5.1a with ϵ=0) are as follows (Ono, 1975):

$$Q_1 = \int_{-\infty}^{\infty} U dX, \tag{5.2a}$$

$$Q_2 = \int_{-\infty}^{\infty} U^2 dX, \tag{5.2b}$$

$$Q_3 = \int_{-\infty}^{\infty} \{ \tfrac{1}{3}U^3 + U\, \mathcal{H}(\tfrac{\partial U}{\partial X}) \} dX. \tag{5.2c}$$

The quantities Q_1 and Q_2 are also integral invariants of the KdV equation. The BDO-Burgers equation exhibits only one time-invariant quantity, Q_1. In all cases where these laws apply, these integral invariants were found to vary by less than 0.1% over the duration of the numerical experiment.

5(a) Solutions of the Benjamin-Davis-Ono equation.

We shall first consider the time-evolution of nonlinear wave disturbances in a horizontally homogeneous inviscid boundary-layer waveguide as described by the unperturbed constant-coefficient Benjamin-Davis-Ono equation. As noted above, BDO solitary waves retain their identity following collision. Interacting BDO solitons have been studied in a series of numerical experiments by Meiss and Pereira (1978) who also showed that both solitary and dispersive waves are created in the evolution of an arbitrary initial disturbance with sech^2 profile. A very detailed analysis of the interaction of BDO solitons has been given by Matsuno (1980). An illustration of the interaction of solitary waves governed by the BDO equation is presented in Figure 6. The nature of the interaction is governed by the ratio of initial amplitudes, U_1 and U_2, of the two interacting solitons. In the example shown in Figure 6 (U_1/U_2=2.8) the solitons exchange identities at the instant of collision without passing through each other. For higher amplitude ratios ($U_1/U_2 > 3+2\sqrt{2}$), the disturbance at the center of interaction is single crested and the solitons pass through each other.

The solitary wave solutions of the BDO equation are also stable under nonlinear interaction with large amplitude dispersive wave components. This is shown by the results of the numerical experiment presented in Figure 7 where a solitary wave is observed to emerge unscathed following a complex interaction with subcritical dispersive waves created in the decay of a long wave of depression.

The behaviour of the general time-dependent solutions of the BDO equation is similar in many respects to that of the coresponding solutions of the classical KdV equation. An excellent description, based on both a theoretical and experimental investigation, of the time-evolution of long nonlinear shallow-water waves governed by the KdV equation may be found in Segur (1973) and Hammack and Segur (1974). The general properties of the time-dependent solutions of the BDO equation which are most relevant to the interpretation of atmospheric wave phenomena may be seen in the numerical solutions presented in Figure 8 for the evolution of an arbitrary initial disturbance in the form of a long wave of elevation. The salient features of the general solutions to the BDO equation may be summarized as follows:

(1) Arbitrary initial disturbances of finite volume evolve asymptotically into a finite number of permanent solitary waves followed by a dispersive oscillatory wave train.

(2) Most of the energy in initial waves of elevation is focussed into the solitary wave components. As a rule, disturbances of this type produce only very minor dispersive wave components. In the illustration shown in Figure 8, the dispersive waves are associated primarily with the decay of the steep trailing edge of the initial wave. Initial waves which decrease more slowly in amplitude behind the leading edge (see, e.g., Figure 11) produce only small amplitude dispersive wave trains.

(3) The speed of the solitary wave components exceeds the linear phase speed, c_0, by an amount proportional to the wave amplitude. The asymptotic solution therefore consists only of a family of amplitude-ordered solitary waves.

(4) Initial disturbances governed by the Benjamin-Davis-Ono equation can evolve into solitary waves of exceptionally large amplitude. For example, in the case of the evolution of the long wave disturbance shown in Figure 8, the ratio of the amplitude of the leading soliton, U_S, at T = 100 to the amplitude of the initial disturbance, U_O, is 2.58. This can be compared with the general solution of the KdV equation where the maximum amplitude of a solitary wave cannot exceed twice the amplitude of the initial disturbance (Peregrine, 1972; Segur, 1973). We have carried out a number of numerical experiments (see, e.g., Figure 9a) which indicate that the limiting value of the ratio U_S/U_O for the BDO equation is, to within the accuracy of our calculations, 3.14 ± 0.05; i.e., it appears that the amplitude of deep-fluid solitary waves can be up to a factor of π larger than the amplitude of the initial disturbance. These calculations therefore show that exceptionally large amplitude solitary wave disturbances may be generated in the evolution of relatively benign initial disturbances. This important feature in the evolution of deep-fluid nonlinear waves does not seem to have been previously recognised. This result has an important bearing on our understanding of hazardous wind shear disturbances (Christie and Muirhead, 1983a, b; 1985) and is clearly of interest to the subject of nonlinear wave-induced deep convection.

(5) Initial waves of depression, i.e., disturbances which are everywhere negative, decay only into dispersive wave components (see Figure 7). Subcritical waves of this type can have large amplitudes for significant periods of time and may, on occasion, play a significant role in the dynamics of the lower atmosphere.

We shall now consider two simple models based on the BDO equation which may, under ideal uniform boundary layer conditions, provide a first-order description of the evolution of nonlinear waves in the lower troposphere. For the first model, we shall suppose that the initial long wave disturbance takes the form of a smooth propagating internal bore marking the transition between two uniform flow states in direct analogy to the classical bore (Rayleigh, 1914) on the surface of shallow water. This model

is suggested by the observation that morning glory waves originate during the evening of the preceeding day over the Cape York Peninsula in the transformation of a deeply-penetrating tropical sea-breeze front. This model may provide a reasonable description of the development of long nonlinear waves under ideal conditions when the generating disturbance is sustained over long periods of time.

Peregrine (1966) showed from a numerical treatment of the Boussinesq equation, the bi-directional equivalent of the KdV equation, that initially smooth bores on the surface of shallow water evolve into undular disturbances. Numerical solutions of the KdV equation for classical shallow-fluid bore waves have also been presented by Vliegenthart (1971) who showed that undulations develop rapidly along the edge of the bore and these in turn evolve into an ever-increasing sequence of discrete solitary waves.

To our knowledge, the evolution of internal deep-fluid bore waves has not been studied previously. The results of a numerical integration of the BDO equation for waves of this type is presented in Figure 9a. For comparison (see Figure 9b), we have also calculated the corresponding bore-wave solutions to the shallow-fluid KdV equation for the same initial conditions. As can be seen from these diagrams, deep-fluid internal bore waves evolve in essentially the same manner as their shallow-fluid counterparts: initially smooth bores develop undulations which evolve into discrete solitary waves. The number of solitary waves created evidently increases without limit as the bore evolves in time. There are, however, significant differences in the evolution patterns described by deep-fluid internal bores and classical shallow-fluid bores. The most important difference lies in the exceptionally large amplitudes of the solitary waves created along the edge of deep-fluid internal bores. As noted above, the amplitudes of solitary waves generated in the evolution of shallow-fluid KdV bores do not exceed twice the amplitude of the parent bore. In contrast, the leading soliton produced in the evolution of a deep-fluid bore eventually attains an amplitude which is apparently a factor of π larger than the amplitude, A_∞,

of the undisturbed bore. These disturbances also differ in morphology. Consider for example a comparison of the detailed evolution patterns as shown in Figure 10 at a time T = 100, where the leading solitons in each disturbance have attained, essentially, their maximum amplitude. This comparison indicates that the transition region in deep-fluid bores tends to be more localized with fewer well-developed solitons. Vliegenthart (1971) noted that the amplitude of the leading solitons in KdV bore waves varies linearly. This linear variation in amplitude is clearly evident in Figure 10 for the first 12 solitary waves in the shallow-fluid disturbance but applies only approximately to the first 3 or 4 solitons in the deep fluid disturbance. In deep-fluid bore waves the energy in the transition zone tends to be concentrated in a few very large amplitude solitary waves. These remarks can be expressed in a more quantitative form by defining an effective transition length, D, by the region along the edge of the bore where the amplitude of the oscillations is at least 10% of that of the leading soliton. For the disturbance shown in Figure 10, the deep-fluid bore has an effective transition zone comprising 7 solitary waves distributed over a region of length 97, in dimensionless units, which may be compared with 14 developing solitons and an effective transition length of 137 in the case of the KdV shallow-fluid bore. In both cases, the distance between individual solitary waves in the transition zone decreases monotonically away from the leading edge. The spacing between the leading solitons and the average wavelength over the transition zone will be useful parameters for the interpretation of experimental data. The scale of both of these parameters is substantially larger for deep-fluid internal bore waves. In the present example, the leading solitons in the BDO bore at T = 100 are separated by a non-dimensional distance of 21.9 and the average wavelength over the effective transition zone is estimated to be 14.0. In the case of the KdV bore the leading soliton separation and average wavelength are 13.2 and 9.7, respectively.

The asymptotic propagation speed, c_b, of bore waves in inviscid fluids is simply given by the speed of the leading soliton. Thus, for BDO bore waves,

$$c_b = c_o + \frac{\pi}{4}\alpha A_\infty \quad , \tag{5.3}$$

and for KdV bores,

$$c_b = c_o + \frac{2}{3}\alpha A_\infty \quad . \tag{5.4}$$

It should be emphasized that the infinitely long internal deep-fluid bore wave considered here represents a highly idealized model for nonlinear atmospheric waves. This model can be expected to provide an accurate description of disturbances which occur only under exceptional atmospheric conditions. Some morning glory wave disturbances certainly do resemble extensive bore waves of this type. However, as emphasized in Section 2, most morning glory disturbances appear to be of finite length. In most cases, the surface winds and pressure recorded behind the main disturbance indicate that the inversion height does not remain elevated but decreases slowly back to the ambient level. On the basis of these observations, we propose that a more suitable model for initial nonlinear wave disturbances is that of a long wave of elevation of effective finite length, L, whose amplitude decreases slowly but continuously behind a maximum amplitude located near the leading edge of the disturbance. This model is consistent with a long, but finite, unsteady wave disturbance created in the transformation during the early evening of a "cut-off" sea-breeze surge as indicated in field observations described by Clarke (1965, 1983a) and Simpson et al. (1977) and in detailed numerical simulations of sea-breeze surges recently reported by Clarke (1984). A typical example of the evolution of a wave of this type as described by the BDO equation is shown in Figure 11. In this case, the initial disturbance evolves almost entirely into a finite number of amplitude-ordered solitary waves. The dispersive wave components have very small amplitudes and play an almost insignificant role in the description of these disturbances. As the wave evolves, the overall length of the disturbance increases continuously as discrete solitary waves form and slowly separate from one another along the leading edge. An exact expression for the number, N_S, of solitons created in the evolution of finite length deep-fluid waves of this type is not

known. However, an approximate estimate of N_S can be found from the square root of the appropriate Ursell number for the initial disturbance. Thus, $N_S \sim \sqrt{U_0 L_0}$ where U_0 and L_0 are the nondimensional amplitude and length of the initial long wave disturbance. For the disturbance illustrated in Figure 11, $N_S \sim 10$. As the volume of the inital disturbance increases, N_S increases without bound and the amplitude of the leading soliton approaches the limiting amplitude for BDO disturbances, πU_0.

The inviscid BDO description of the evolution of long finite length nonlinear wave disturbances outlined above provides a reasonable description of many of the features of long nonlinear atmospheric wave disturbances, especially during the earlier stages of evolution involving the formation and growth of solitary waves. This relatively simple model is however subject to serious criticism since it fails to describe the decay and disintegration of these disturbances. Furtherfore, in some cases (see Figures 2b and 3d) only one large amplitude solitary wave is observed to develop along the leading edge of the disturbance contrary to the predictions of this relatively simple model. As we shall see, turbulent dissipation plays an important role in the evolution of these disturbances and must be included in a more realistic theoretical treatment of the properties of these guided nonlinear waves.

5(b) Solutions of the Benjamin-Davis-Ono-Burgers equation.

The description of the evolution of deep-fluid long wave disturbances is modified substantially when a term for turbulent dissipation is included in the governing equation. We shall first consider the effect of turbulent friction on the properties of simple deep-fluid internal bore waves as described by the BDO-Burgers evolution equation (5.1). Internal bores in either deep or shallow inviscid fluids (Figure 9) evolve continuously in time as an ever-increasing number of solitary waves are created in the transition zone along the leading edge. When turbulent dissipation is included in the treatment of the classical shallow fluid bore wave, initial bore wave disturbances

of arbitrary form are found to evolve rapidly to a stable time-independent solution which may be smooth or undular depending upon the degree of frictional dissipation (Canosa and Gazdag, 1977). This classical stationary bore or 'shock' wave solution to the steady-state KdV-Burgers equation has been studied in the phase plane as a model for weak shock waves in plasmas by Grad and Hu (1967), and also by Johnson (1970, 1972) as a model for undular bores on a shallow viscous fluid. Johnson numerically integrated the steady-state KdV-Burgers equation, and also derived asymptotic solutions, corresponding to either weak or strong damping, for the stationary bore-wave transition between uniform upstream and downstream flow states. Detailed accounts of the time-independent solution of the KdV-Burgers equation have also been given by Jeffrey and Kakutani (1972), Witham (1974), Karpman (1975), and, as a proposed model for the morning glory, by Egger (1983, 1984). Following Johnson (1970), the properties of the stationary bore wave solution of the KdV-Burgers equation,

$$\frac{\partial U}{\partial T} + U\frac{\partial U}{\partial X} + \frac{\partial^3 U}{\partial X^3} - \epsilon\frac{\partial^2 U}{\partial X^2} = 0 \qquad (5.5)$$

are determined by the value of the parameter

$$m = 2\epsilon/\sqrt{2/U_\infty} \quad , \qquad (5.6)$$

where U_∞ is the dimensionless amplitude of the undisturbed bore at $X \to -\infty$. When $m < 4$, dispersion dominates and the resulting stationary bore wave is undular. If $m > 4$, the influence of turbulent dissipation exceeds that of dispersion and the bore profile is monotonic. In the limit where dispersive effects are negligible, the stationary bore solution is given by the Taylor shock profile (Taylor, 1910),

$$U(X) = \frac{U_\infty}{2}\left\{1 - \tanh\left[\frac{U_\infty X}{4\epsilon}\right]\right\} \qquad (5.7)$$

The corresponding stationary bore solutions for the BDO-Burgers equation have not been studied previously. As will be seen, these steady solutions are exceptionally stable, even under strongly nonlinear perturbation, provided the upstream and

downstream boundary conditions are constant. These stationary deep-fluid bore waves may provide a reasonable model for long nonlinear atmospheric wave disturbances which occur under conditions where turbulent dissipation is significant and where the increased inversion depth far upstream from the edge of the bore is sustained for substantial periods of time.

It can be anticipated that the stationary internal deep-fluid bore waves described by the BDO-Burgers equation are similar in many respects to the corresponding well-known solutions of the shallow-fluid KdV-Burgers equation. The steady solutions to the BDO-Burgers equation have been determined by numerically integrating (5.1) for an initial positive step function of amplitude U_0 subject to the boundary conditions: $U(-\infty) = U_0$, $U(+\infty) = 0$. Some typical results of these calculations are presented in Figures 12(a) and 12(b) for both weak ($\epsilon = 0.1$) and strong ($\epsilon = 2.0$) turbulent dissipation coefficients. It can be seen from these diagrams that the initially time-dependent bore-wave solution rapidly converges to the steady-state solution. As in the case of KdV-Burgers equation, when the damping coefficient is small, the stationary internal bore wave solution is dominated by dispersive effects and the solution (Figure 9a) takes the form of an oscillatory bore. If, on the other hand, turbulent dissipation dominates over dispersion, the stationary solution is monotonic and approaches the Taylor shock profile (5.7) in the limit where dispersive effects are negligible. We have also evaluated the corresponding steady-state solutions to the KdV-Burgers equation. It is worth noting that the effects of dispersion are much stronger in the case of the BDO-Burgers equation. This is reflected in the observation that the transition from an oscillatory bore to a monotonic shock occurs at a much larger value of the dissipation coefficient. The oscillations along the edge of weakly-damped deep-fluid stationary bores are also larger in amplitude, but fewer in number, than those in the corresponding KdV-Burgers solution for the same degree of turbulent dissipation. The effective length of the transition zone in both deep-fluid and classical stationary bore waves are approximately the same, but the wavelength for

undular disturbances, which is now fairly uniform over the transition region, is substantially larger in the case of deep-fluid internal bores. For example, the wavelength of the oscillations along the edge of the stationary deep-fluid bore wave illustrated in Figure 12(a) is approximately 35% longer than the wavelength of the equivalent shallow-fluid KdV-Burgers disturbance.

It can be shown directly by applying the upstream boundary condition to the steady-state equations that stationary bore waves in either deep or shallow fluids propagate at a supercritical constant speed given by

$$c = c_o + \tfrac{1}{2} \alpha A_\infty \qquad (5.8)$$

The propagation speed therefore depends only on the bore amplitude and waveguide structure and is independent of the degree of turbulent dissipation. Stationary bore waves therefore propagate slower than the asymptotic frictionless bore waves described by either the KdV or BDO equations (see 5.3 and 5.4).

The stationary internal bore-wave solutions of the BDO-Burgers equation appears to be exceptionally stable to large-amplitude waveform perturbations. This is illustrated by the numerical experiment presented in Figure 13 for the evolution of an initial bore transition in the form of an irregular wave of elevation followed by a temporary increase in amplitude to a value which exceeds the fixed amplitude determined by the upstream boundary condition. As can be seen from the diagram, this fairly complex initial bore wave transition converges rapidly to the stationary internal deep-fluid bore specified by the constant upstream and downstream boundary conditions. Evidently, both the asymptotic waveform and speed of the BDO-Burgers (and also the KdV-Burgers solution; see, Canosa and Gazdag, 1977) bore-wave solution between uniform flow states are independent of the nature of the initial bore transition. It can therefore be concluded that initial internal bores of arbitrary shape which connect two steady deep-fluid flow regimes will evolve rapidly into the stationary oscillatory or monotonic bore-wave solutions of the time-independent BDO-Burgers equation.

On occasion, very extensive nonlinear wave disturbances (see Figure 2), with 8 or

more partially resolved solitary waves, are observed over northern Australia. Relatively smooth, quasi-stationary disturbances in the form of monotonic bore waves are also seen on occasion. Both of these types of nonlinear wave disturbances have many features in common with the class of internal deep-fluid bore waves described by the steady-state BDO-Burgers equation. It has been emphasized, however, that nonlinear wave disturbances often appear to have limited spatial extent. In this case a description of the properties of these commonly occurring disburbances in terms of a stationary internal bore wave model is no longer possible. We therefore propose that a more suitable model for nonlinear wave disturbances of this type which are subject to turbulent dissipation is that described by the time-evolution of an initially smooth, long, but finite-length wave of elevation, as governed by the deep fluid BDO-Burgers equation.

The propagation characteristics of finite-length initial wave disturbances differ substantially from those of infinitely long internal bore wave disturbances when turbulent frictional dissipation is significant. Solitary waves may also form along the leading edge of these finite-volume disturbances and the degree to which they develop depends again on the relative influence of turbulent dissipation and dispersion. The principal features in the evolution of finite-length disturbances, as governed by the BDO-Burgers equation, may be seen in the numerical experiments presented in Figure 14 for the same initial disturbance as that in Figure 11. In contrast with the steady solution for an idealized infinitely long internal bore wave, the solution for the vertical displacement in this case is always time-dependent. For modest dissipation, solitary waves develop rapidly along the leading edge of the disturbance and increase in amplitude to a maximum which is less than that described by the corresponding stationary bore wave solution for the same degree of turbulent dissipation. From this point on, the undular wave profile has almost constant form but the amplitude of the disturbance decays continuously as energy is dissipated by turbulent boundary friction. When dissipation dominates over dispersion, the formation of solitary waves is

suppressed and the initial disturbance slowly increases in length as it decays in amplitude. It is worth noting that smaller amplitude solitary waves and the oscillatory dispersive wave components which arise in the evolution of finite-length waves of elevation in the absence of frictional dissipation (see e.g., Figures 8 and 11) are strongly attenuated by a relatively small degree of turbulent damping. The leading wave components in finite volume disturbances of this type propagate, at least during the earlier stages of evolution, at supercritical speeds which are comparable to, though slightly smaller than, the speed of stationary internal bore waves of the same initial amplitude. Since long waves of this type in viscous fluids produce negligible dispersive wave components, the overall length of the disturbance during its early development is determined by the approximate expression

$$L(t) \simeq L(0) + \tfrac{1}{2}\alpha A_0 t. \qquad (5.9)$$

6. Nonlinear Wave Propagation in an Inhomogeneous Waveguide

The BDO-Burgers equation with constant coefficients appears to provide a reasonably satisfactory description of many of the essential features in the evolution of long nonlinear wave disturbances in the lower atmosphere. Conditions can occur however in the real atmosphere where the assumption of a uniformly constant eddy diffusivity coefficient is no longer justified. We shall therefore examine in this section the influence on nonlinear wave propagation of spatial and temporal variations in the degree of turbulent frictional dissipation. Two specific problems which have a direct bearing on the interpretation of experimental observations will be addressed. In the first part of this section we present the results of a numerical study of nonlinear wave propagation under conditions where the degree of turbulent dissipation varies along the propagation path. This is followed in Section 6(b) by a brief discussion of shear instability in the leading solitary wave components and the subsequent influence of the resulting increase in turbulence on the development of the residual long wave

disturbance.

6(a) Horizontal variations in waveguide structure

The calculations presented in Section 5(b) show that the morphology of long nonlinear wave disturbances depends sensitively on the degree of turbulent boundary friction. It can therefore be anticipated that the evolution of finite-amplitude waves in the lower atmosphere will be strongly influenced by horizontal variations in the Chezy friction coefficient. In order to study this effect we have carried out a number of numerical experiments in which a propagating long wave disturbance is subjected to a variation in turbulent boundary friction such as might be encountered for example when a nonlinear wave disturbance propagates over a land-sea boundary. In the first example (see Fig. 15) a long smooth finite length nonlinear wave is allowed to evolve initially under frictionless waveguide conditions into an amplitude-ordered family of solitary waves as described by the BDO equation. At T = 120 this well-resolved solitary wave group is subjected to the onset of strong turbulent boundary friction. As can be seen from the diagram, the well-developed solitary wave structure is rapidly eroded away under the influence of turbulent frictional damping and the resulting long wave disturbance continues to slowly increase in length as it decays away in amplitude. It is worth noting that an increase in the degree of turbulent friction also results in a significant and rapid decrease in the speed of propagation. The results of this calculation therefore indicate that the sharp bend in morning glory wave cloud lines at the point where the cloud lines intersect the sea-land boundary as described by Smith and Page (1985) can be attributed, at least in part, to a decrease in the speed of propagation over land resulting from increased turbulent boundary friction.

A second illustration of the influence of a sudden variation in the degree of turbulent frictional damping is presented in the evolution pattern shown in Figure 16. In this case a smooth finite-length disturbance evolves initially under the influence of

strong frictional dissipation as described by the BDO-Burgers equation. The disturbance slowly decreases in amplitude until T = 120, at which point the eddy diffusivity coefficient is reduced to zero and the subsequent evolution of the disturbance is described by the inviscid BDO equation. The evolution of the long nonlinear wave distubance proceeds in this case as expected. Prior to the sudden decrease in boundary friction the disturbance evolves only slowly as described in Section 5(b) and when frictional damping is removed the disturbance rapidly increases in speed as solitary waves develop along the leading edge.

The two examples presented here of nonlinear wave propagation in an inhomogeneous waveguide serve to illustrate the principal effects which result from horizontal variations in the degree of turbulent frictional dissipation. We have also carried out a number of numerical experiments in which the eddy diffusivity coeffiecient varies continuously over the course of the experiment. These results will not be described in detail as they are similar in most respects to those described above.

6(b) Solitary-wave-induced turbulence

Up to this point, all of the calculations have been based on the assumption that the Chezy turbulent friction coefficient is independent of the nature of the nonlinear wave motions. This may prove to be a reasonable approximation when the Richardson number throughout the environmental shear flow is large and when the amplitude of the waves is small. It must, however, be expected that the Chezy coefficient will depend on both the amplitude and period of the wave motion and that wave-induced variations in the frictional dissipation rate may have a significant influence on the evolution of these disturbances. A nonlinear wave-induced variation in the Chezy coefficient is clearly indicated by observations of morning glory wave phenomena and other closely-related nonlinear wave disturbances. For example, the leading solitary

wave roll cloud formation in visible morning glory disturbances is often observed (Christie et al., 1983b; Smith and Morton, 1984) to be extremely smooth along the leading edge and highly turbulent along the trailing edge. This wave-induced turbulence is apparently the result of the onset of Kelvin-Helmholtz instability near the crest of the wave. Subsequent solitary wave roll clouds are almost invariably observed to be highly turbulent which indicates that the wave-generated turbulence decays slowly relative to the characteristic time-scale of these disturbances. An excellent aerial photograph of a morning glory disturbance which illustrates the highly turbulent nature of the cloud lines in the wake of the leading solitary roll cloud formation is given in Figure 2 of Smith and Morton (1984). Solitary wave induced turbulence has been observed in laboratory experiments (J. Simpson, private communication quoted in Smith and Morton, 1984; see also, Maxworthy, 1980) and has been directly observed in the atmosphere by Doviak and Ge (1984) using the KTVY tower instrumented by the National Severe Storms Laboratory at Norman, Oklahoma. Further evidence for wave-induced turbulence is provided by the observation of an increase in surface temperature due to mixing which almost invariably occurs in the wake of the leading solitary wave in well-developed morning glory disturbances. It must be expected that wave-induced turbulence associated with the leading solitary wave components will have a substantial influence on the development of the residual wave disturbance.

As a first step in the study of this complex process, we present the results of a numerical experiment (Figure 17) in which the effect of wave-induced turbulence is accounted for by an increase in the Chezy friction coefficient in the wake of the leading solitary wave. In this simple first approximation we assume that the wave-induced frictional component appears initially when the leading solitary wave amplitude, A_0, reaches a critical amplitude, A_c, corresponding to a critical local Richardson number, and that once this critical amplitude is reached the degree of wave-induced frictional damping in the wake of the leading solitary wave is

proportional to A_0-A_C. Thus, in this very simple model, the leading solitary wave is subject to a constant damping coefficient $\epsilon = \epsilon_0$ characteristic of the ambient environment and the residual disturbance develops under the influence of a time-dependent coefficient,

$$\epsilon(t) = \epsilon_0 + \epsilon_1(A_0(t)-A_C) \quad . \tag{6.1}$$

The results of this calculation as illustrated in Figure 17 show that the turbulence field produced in the wake of the leading solitary wave can limit or inhibit completely the development of further solitary waves in the residual disturbance. This model therefore provides an explanation for observations of nonlinear wave phenomena (Figures 2b and 3d) in which only one large amplitude solitary wave developes along the leading edge of the parent disturbance. It should be emphasized, however, that this model over-simplifies considerably the dynamics of wave-induced turbulent dissipation. This simple model is presented here to illustrate the principal features in the evolution of long nonlinear wave disturbances which arise when shear instabilities occur in the leading solitary wave component. Other more realistic models for this complex process are currently under investigation and the results will be reported elsewhere.

7. Concluding Remarks

This paper has been concerned with the theoretical description of the evolution of long nonlinear wave disturbances in the atmospheric boundary layer. A number of realistic models for these disturbances have been developed within the framework of either the deep-fluid Benjamin-Davis-Ono evolution equation for ideal homogeneous waveguide conditions where frictional processes are negligible, or the BDO-Burgers evolution equation for conditions where turbulent dissipation plays a significant role. The evolution of a wide variety of initial disturbances, including infinitely long internal bore waves and long waves of finite volume has been studied in considerable

detail. These models clearly explain the essential features in the observed evolution of morning glory waves and other similar nonlinear atmospheric wave phenomena. It should be emphasized, however, that the theory is limited to a description of waves of modest amplitude and the present results will be quantitatively unreliable for very large amplitude waves with regions of recirculating fluid (Tung et al. 1982). The waveguide models chosen to illustrate this theory are also over-simplified in many respects. A more complete description of the evolution of these disturbances should include a detailed analysis of the influence of spatial and temporal variations in the waveguide density and shear structure.

References

Ablowitz, M.J. and Segur, H. 1980. Long internal waves in fluids of great depth. Studies in Appl. Math., 62, 249-262.

Benjamin, T.B., 1966. Internal waves of finite amplitude and permanent form. J. Fluid Mech., 25, 241-270

Benjamin, T.B., 1967. Internal waves of permanent form in fluids of great depth. J. Fluid Mech., 29, 559-592.

Benney, D.J., 1966. Long nonlinear waves in fluid flows. J. Math. and Phys., 45, 52-63.

Canosa, J. and Gazdag, J., 1977. The Korteweg-de Vries-Burgers Equation. J. Computational Phys., 23, 393-403.

Case, K.M., 1978. The N-soliton solution of the Benjamin-Ono equation. Proc. Nat. Acad. Sci. U.S.A., 75, 3562-3563.

Chen, H.H., Lee, Y.C. and Pereira, N.R., 1979. Algebraic internal wave solitons and the integrable Calogero-Moser-Sutherland N-body problem. Phys. Fluids, 22, 187-188.

Christie, D.R., Muirhead, K.J. and Clarke, R.H., 1981. Solitary waves in the lower atmosphere. Nature, 293, 46-49.

Christie, D.R., Muirhead, K.J. and Hales, A.L., 1978. On solitary waves in the atmosphere. J. Atmos. Sci., 35, 805-825.

Christie, D.R., Muirhead, K.J. and Hales, A.L., 1979. Intrusive density flows in the lower troposphere: A source of atmospheric solitons. J. Geophys. Res., 84, 4959-4970.

Christie, D.R. and Muirhead, K.J., 1981. Observations of solitary atmospheric waves over Northern Australia. Physics for Australia's Development, Second Applied Physics Conference, Australian Institute of Physics, Melbourne, 463-466.

Christie, D.R. and Muirhead, K.J., 1983a. Solitary waves : a hazard to aircraft operating at low altitudes. Aust. Met. Mag., 31, 97-109.

Christie, D.R. and Muirhead, K.J., 1983b. Solitary waves: a low-level wind shear hazard to aviation. International J. Aviation Safety, 1, 169-190.

Christie, D.R. and Muirhead, K.J., 1985. Solitary waves and low-altitude wind shear in Australia. Aviation Safety Digest, 123, 3-9.

Clarke, R.H., 1965. Horizontal mesoscale vortices in the atmosphere. Aust. Met. Mag., 50, 1-25.

Clarke, R.H., 1983a. Fair weather nocturnal inland wind surges and atmospheric bores: Part I Nocturnal wind surges. Aust. Met. Mag., 31, 133-145.

Clarke, R.H., 1983b. Fair weather nocturnal inland wind surges and atmospheric bores: Part II Internal atmospheric bores in northern Australia. Aust. Met. Mag., 31, 147-160.

Clarke, R.H., 1984. Colliding seabreezes and atmospheric bores: Two-dimensional numerical studies. Aust. Met. Mag., 32, 207-226.

Clarke, R.H., 1986. Several atmospheric bores and a cold front over southern Australia. Aust. Met. Mag., 34, 65-76.

Clarke, R.H., Smith, R.K. and Reid, D.G., 1981. The morning glory of the Gulf of Carpentaria: an atmospheric undular bore. Mon. Wea. Rev., 109, 1726-1750.

Crook N.A. and Miller, M.J., 1985. A numerical and analytical study of atmospheric undular bores. Quart. J.R. Met. Soc., 111, 225-242.

Crook, N.A., 1986. The effect of ambient stratification and moisture on the motion of atmospheric undular bores. J. Atmos. Sci. 43, 171-181.

Davis, R.E. and Acrivos, A., 1967. Solitary internal waves in deep water. J. Fluid Mech., 29, 593-607.

Doviak, R.J. and Ge, R., 1984. An atmospheric solitary gust observed with a Doppler radar, a tall tower and a surface network. J. Atmos. Sci., 41, 2559-2573.

Drake, V.A., 1984a. A solitary wave disturbance of the marine boundary layer over Spencer Gulf revealed by radar observations of migrating insects. Aust. Met. Mag. 32, 131-135.

Drake, V.A., 1985. Solitary wave disturbances of the nocturnal boundary layer revealed by radar observations of migrating insects. Boundary Layer Meteorol. 31, 269-286.

Egger, J., 1983. The morning glory: a nonlinear wave phenomenon. In Mesoscale Meteorology - Theories, Observations and Models, ed. D.K. Lilly and T.Gal-Chen. Reidel, Dordrecht, pp. 339-353.

Egger, J. 1984. On the theory of the morning glory. Beitr. Phys. Atmosph. 57, 123-134.

Grad, H. and Hu, P.N. 1967. Unified shock profile in a plasma. Phys. Fluids, 10, 2596-2602.

Goncharov, V.P. and Matveyev, A.K., 1982 Observations of nonlinear waves on an atmospheric inversion. Izv. Acad. Sci. USSR Atmos. Oceanic Phys., Engl. Transl., 18, 61-64.

Grimshaw, R., 1980/81. Solitary waves in a compressible fluid. Pageoph., 119, 780-797.

Grimshaw, R., 1981a. Evolution equations for long, nonlinear internal waves in stratified shear flows. Studies in Appl. Math., 65, 159-188.

Grimshaw, R., 1981b. A second-order theory for solitary waves in deep fluids. Phys. Fluids, 24, 1611-1618.

Grimshaw, R., 1981c. Slowly varying solitary waves in deep fluids. Proc. R. Soc. Lond., A376, 319-332.

Grimshaw, R., 1982. Solitary waves in density stratified fluids. In Nonlinear Deformation Waves, ed. U. Nigul and J. Engelbrecht, IUTAM Symposium, Tallinn. Springer, pp.431-447.

Grimshaw, R., 1985. Evolution equation for weakly nonlinear, long internal waves in a rotating fluid. Studies in Appl. Math., 73, 1-33.

Hammack, J.L. and Segur, H., 1974. The Korteweg-de Vries equation and water waves. Part 2. Comparison with experiments. J. Fluid Mech., 65, 289-314.

Haase, S. and Smith, R.K., 1984. Morning glory wave clouds in Oklahoma: a case study. Mon. Weath. Rev., 112, 2078-2089.

Hirota, R., 1971. Exact solution of the Korteweg-de Vries equation for multiple collisions of solitons. Phys. Rev. Lett., 27, 1192-1194.

Jeffrey, A. and Kakutani, T., 1972 Weak nonlinear dispersive waves : A discussion centered around the Korteweg-de Vries equation SIAM Review, 14, 582-643.

Johnson, R.S., 1970. A non-linear equation incorporating damping and dispersion. J. Fluid Mech., 42, 49-60.

Johnson, R.S., 1972. Shallow water waves on a viscous fluid - the undular bore. Phys. Fluids, 15, 1693-1699.

Joseph, R.J., 1977. Solitary waves in a finite depth fluid. J. Phys. A: Math. Gen., 10, L225-227.

Karpman, V.I., 1975. Non-linear Waves in Dispersive Media. Oxford : Pergamon, 186 pp.

Koop, C.G. and Butler G., 1981. An investigation of internal solitary waves in a two-fluid system. J. Fluid Mech., 112, 225-251.

Kubota, T., Ko, D.R.S. and Dobbs, L.D., 1978. Propagation of weakly nonlinear internal waves in a stratified fluid of finite depth. A.I.A.A.J. Hydronautics, 12, 157-165.

Maslowe, S.A. and Redekopp, L.G., 1979. Solitary waves in stratified shear flows. Geophys. Astrophys. Fluid Dynamics, 13, 185-196.

Maslowe, S.A. and Redekopp, L.G., 1980. Long nonlinear waves in stratified shear flows. J. Fluid Mech., 101, 321-348.

Matsuno, Y., 1979. Exact multi-soliton solution of the Benjamin-Ono equation. J. Phys. A: Math. Gen., 12, 619-621.

Matsuno, Y., 1980. Interaction of the Benjamin-Ono solitons. J. Phys. A: Math. Gen., 13, 1519-1536.

Maxworthy, T., 1980. On the formation of nonlinear internal waves from the gravitational collapse of mixed regions in two and three dimensions. J. Fluid Mech., 96, 47-64.

Meiss, J.D. and Pereira, N.R. 1978. Internal wave solitons. Phys. Fluids, 21, 700-702; 22, 201.

Miura, R.M., Gardner, C.S., and Kruskal, M.D., 1968. Korteweg-de Vries equation and generalizations. II. Existence of conservation laws and constants of motion. J. Math. Phys., 9, 1204-1209.

Mulroney, D.T., 1984. Roll clouds over the Somerville-Tyabb area. Meteorology Australia, 3, 4-5.

Nakamura, A., 1979. Bäcklund tranform and conservation laws of the Benjamin-Ono equation. J. Phys. Soc. Japan, 47, 1335-1340.

Noonan, J.A. and Smith, R.K., 1985. Linear and weakly nonlinear internal wave theories applied to 'morning glory' waves. Geophys. Astrophys. Fluid Dynamics, 33, 123-143

Noonan, J.A. and Smith, R.K., 1986. Sea breeze circulations over Cape York Peninsula and the generation of the Gulf of Carpentaria cloud line disturbances. J. Atmos. Sci., 43, 1679-1693.

Ono, H., 1975. Algebraic solitary waves in stratified fluids J. Phys. Soc. Japan, 39, 1082-1091.

Peregrine, D.H., 1966. Calculations of the development of an undular bore. J. Fluid Mech., 25, 321-330.

Peregrine, D.H., 1972. Long waves in two and three dimensions. Proc. Symp. on Long Waves, University of Delaware, Sept. 10-11, 1970, pp. 63-90.

Periera, N.R. and Redekopp, L.G., 1980. Radiation damping of long, finite-amplitude internal waves. Phys. Fluids, 23, 2182-2183.

Physick, W., 1987. Observations of a solitary wave train at Melbourne, Australia, To appear Aust. Met. Mag, 35.

Rayleigh, Lord, 1914. On the theory of long waves and bores. Proc. Roy. Soc. A, 90, 324-328.

Redekopp, L.G., 1980. Similarity solutions of some two-space- dimensional nonlinear wave evolution equations. Studies in Appl. Math., 63, 185-207.

Scorer, R.S., 1949. Theory of waves in the lee of mountains. Quart. J. Roy. Met. Soc., 75, 41-56.

Segur, H., 1973. The Korteweg-de Vries equation and water waves : Solutions of the equation, 1. J. Fluid Mech., 59, 721-736.

Shreffler, J.H. and Binkowski, F.S., 1981. Observations of pressure jump lines in the Midwest, 10-12 August 1976. Mon. Wea. Rev., 109, 1713-1725.

Simpson, J.E., Mansfield, D.A. and Milford, J.R., 1977. Inland penetration of sea breeze fronts. Quart. J. Roy. Met. Soc., 103, 47-76.

Smith, R.K., 1986. Evening glory wave-cloud lines in northwestern Australia. Aust. Met. Mag., 34, 27-33.

Smith, R.K., Crook, N. and Roff, G., 1982. The Morning Glory: An extraordinary atmospheric undular bore. Quart. J.R. Met. Soc., 108, 937-956.

Smith, R.K., Coughlan, M.J. and Lopez, J.-L., 1986. Southerly noctural wind surges and bores in northeastern Australia. Mon. Wea. Rev., 114, 1501-1518.

Smith R.K. and Morton, B.R., 1984. An observational study of northeasterly 'morning glory' wing surges. Aust. Met. Mag., 32, 155-175.

Smith, R.K. and Page, M.A., 1985. Morning glory wind surges and the Gulf of Carpentaria cloud line of 25-26 October 1984. Aust. Met. Mag., 33, 185-194.

Taylor, G.I., 1910. The conditions necessary for discontinuous motion in gases. Proc. Roy. Soc. A, 84, 371-377.

Tung, K.-K., Chan, T.F. and Kubota, T., 1982. Large amplitude internal waves of permanent form. Studies Appl. Math., 66, 1-44.

Tung, K.-K., Ko, D.R.S. and Chang, J.J., 1981. Weakly nonlinear internal waves in shear. Studies Appl. Math., 65, 189-221.

Vliegenthart, A.C., 1971. On finite difference methods for the Korteweg-de Vries equation. J. Eng. Math., 5, 137-155.

Whitham, G.B., 1974. Linear and Nonlinear Waves. New York: Wiley & Sons, 636 pp.

Zabusky, N.J. and Kruskal, M.D., 1965. Interaction of "solitons" in a collisionless plasma and the recurrence of initial states. Phys. Rev. Lett., 15, 240-243.

Figure Captions

Figure 1. Surface micropressure records corresponding to amplitude - ordered morning glory solitary wave disturbances at the Edward River Mission on the eastern side of the Gulf of Carpentaria. Onset times, source azimuths and propagation speeds are as follows: (a) 2152 EST (Eastern Standard Time), Sept. 15, 1983, 28°, 5.9 m/s; (b) 2120 EST, Sept. 18, 1983, 31°, 6.3 m/s; (c) 2117 EST, Sept. 24, 1983, 35°, 7.2 m/s.

Figure 2. Typical surface micropressure signatures of extensive morning glory disturbances recorded at various locations around the south-eastern margin of the Gulf of Carpentaria. Onset times, source azimuths and propagation speeds are as follows: (a) 0323 EST Oct. 3, 1983, 77°, 10.2 m/s; (b) 0650 EST, Oct. 3, 1983, 79°, 10.6 m/s; (c) 0649 EST, Oct. 9, 1983, 51°, 17.1 m/s; (d) 0539 EST, Oct. 15, 1983, 33°, 8.8 m/s. The event shown in (b) represents a later stage in the development of the event illustrated in (a). Events (b) and (c) were accompanied by solitary wave roll cloud formations. The flattened crest in the micropressure profile of the leading solitary wave in events (b) and (c) is a manifestation of closed circulation in the relative streamline pattern.

Figure 3. Examples of typical micropressure records corresponding to relatively short-lived morning glory nonlinear wave disturbances. Onset times, source azimuths and propagation speeds are respectively: (a) 0140 EST, Sept. 26, 1983, 92°, 11.3 m/s; (b) 0020 EST, Sept. 28, 1983, 94°, 10.0 m/s; (c) 0028 EST, Oct. 23, 1983, 96°, 11.7 m/s; (d) 0741 EST, Oct 27, 1983, 34°, 14.7 m/s. All of these events occurred as clear-air disturbances with the exception of event (d) which was accompanied by a single spectacular solitary wave roll cloud formation in the Burketown area.

Figure 4. Inner and outer relative streamline patterns, surface perturbation pressure and wind components corresponding to a solitary wave of amplitude a = 350 m propagating in a surface based inversion waveguide described by model b with n=1, $u_1=u_2=0$, $\Delta\rho=0$, h=500 m, and constant Brunt-Väisälä period T_N=4.1 min. Values of the non-dimensional stream function are shown at left in the streamline diagram. ΔP_T is the total perturbation pressure at the surface.

Figure 5. Relative streamline pattern, surface perturbation pressure and wind components for an amplitude-ordered family of solitary waves propagating in an inversion waveguide described by model b with n=1, $u_1=u_2=0$, $\Delta\rho=0$, h=500 m, and T_N=4.8 min. The hydrodynamic contribution to the total surface perturbation pressure (solid curve) is shown by the dashed curve.

Figure 6. Interaction of solitary waves governed by the Benjamin- Davis-Ono equation. The last trace has been reproduced separately for clarity. The co-ordinate system in this illustration and in all subsequent illustrations moves at the critical or linear phase speed. In this frame of reference, solitary waves propagate to the right and subcritical dispersive wave components propagate to the left. Units are nondimensional.

Figure 7. Numerical integration of the Benjamin-Davis-Ono equation illustrating the stability of a solitary wave under strongly nonlinear interaction with large amplitude subcritical dispersive waves created in the evolution of an initially smooth long wave of depression.

Figure 8. Numerical solution of the BDO equation illustrating the evolution of a long square wave of elevation into a finite number of amplitude-ordered solitons followed by a subcritical dispersive wave train.

Figure 9. (a) Numerical integration of the BDO equation for an initially smooth deep-fluid internal bore wave.

(b) Corresponding solution of the shallow-fluid KdV equation for the same initial bore wave condition used in the calculations shown in (a).

Figure 10. Detailed comparison of (a) the structure of a deep-fluid internal bore wave with (b) the structure of a shallow-fluid bore wave corresponding to the same solutions as those shown in Figure 9 at T=100.

Figure 11. Solution of the BDO equation for an initial model disturbance for atmospheric waves in the form of a long, but finite-length, wave of elevation. The inversion height behind the leading edge of the disturbance at T=0 decreases slowly, but continuously, to the ambient inversion level.

Figure 12. Numerical integration of the BDO-Burgers equation for an initally smooth deep-fluid internal bore with (a) weak turbulent dissipation, $\epsilon = 0.1$ and (b) strong turbulent dissipation, $\epsilon = 2.0$. Stationary internal bore wave solutions are well established by T = 80 in both cases.

Figure 13. Illustration of the stability of the BDO-Burgers stationary internal bore wave solution to large amplitude perturbations. This calculation shows that arbitrary transition wave forms connecting different uniform flow states converge rapidly to the unique time-independent bore wave solution specified by the uniform boundary conditions and the degree of turbulent dissipation. In this example $\epsilon = 0.1$. The stationary wave solution is established by T = 140.

Figure 14. Numerical integration of the BDO-Burgers equation for an initial model disturbance for finite-length atmospheric waves with (a) $\epsilon = -0.05$ and (b) $\epsilon = -0.5$.

Figure 15. Illustration of the influence of an increase in the degree of turbulent boundary friction on the evolution of a long initially smooth finite-length wave of elevation. For $T < 120$, $\epsilon = 0$; for $T > 120$, the disturbance is subject to strong dissipation with $\epsilon = -0.5$.

Figure 16. Numerical integration of the BDO-Burgers equation illustrating the effect of a decrease in turbulent dissipation on the evolution of an initially smooth finite-length long wave of elevation. In this example $\epsilon = -0.5$ for $t < 120$. For $T > 120$, $\epsilon = 0$.

Figure 17. Model calculation illustrating the influence of wave-induced turbulent dissipation on the evolution of long wave disturbances in the lower atmosphere. In this example the turbulent dissipation coefficient in the BDO-Burgers equation is given by the spatially and temporally varying coefficient specified by (6.1) with $\epsilon_0 = 0.05$, $\epsilon_1 = 0.5$ and a critical amplitude, A_c, for the onset of wave-induced turbulence which is 20% larger than the maximum amplitude of the initial disturbance.

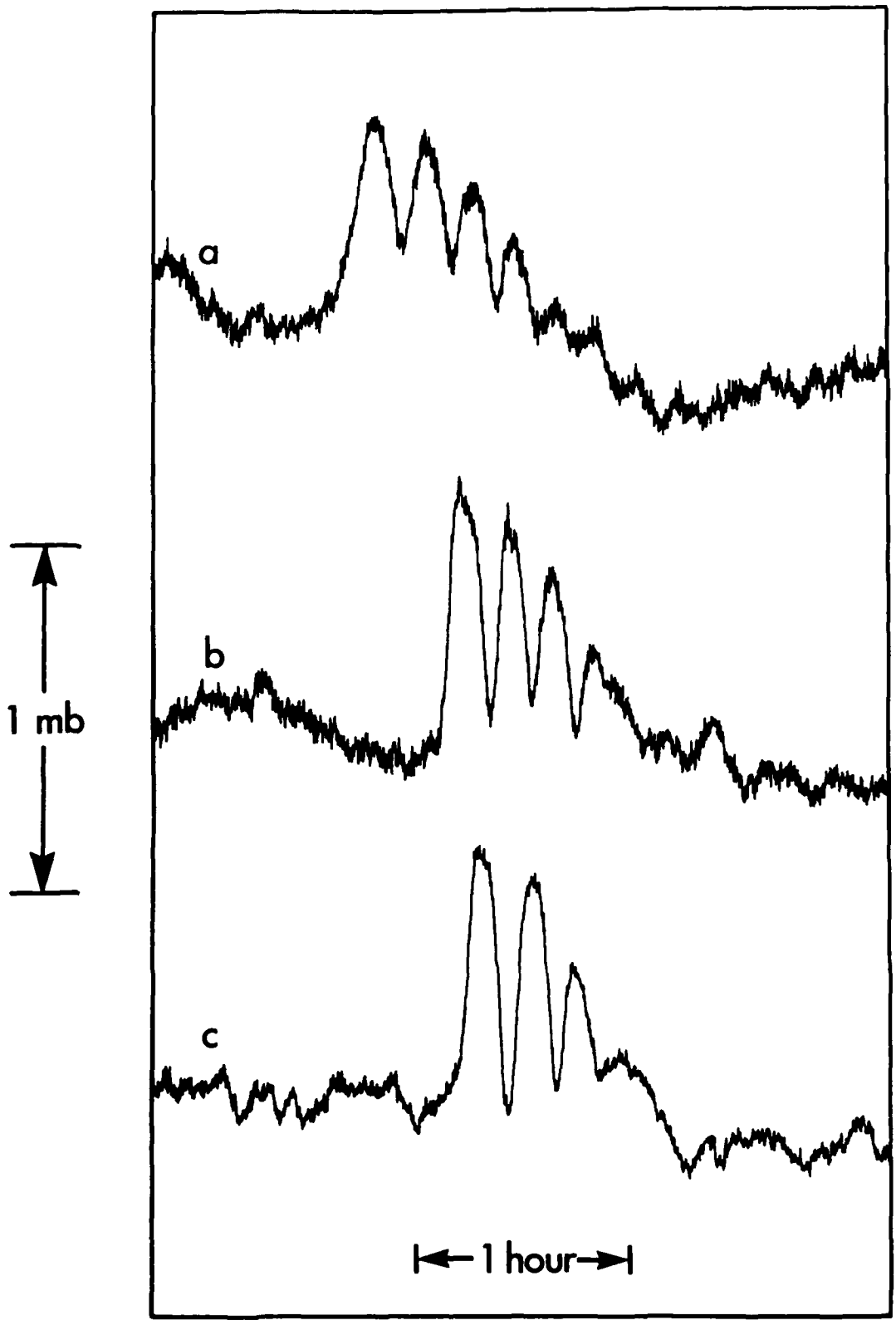

Figure 1

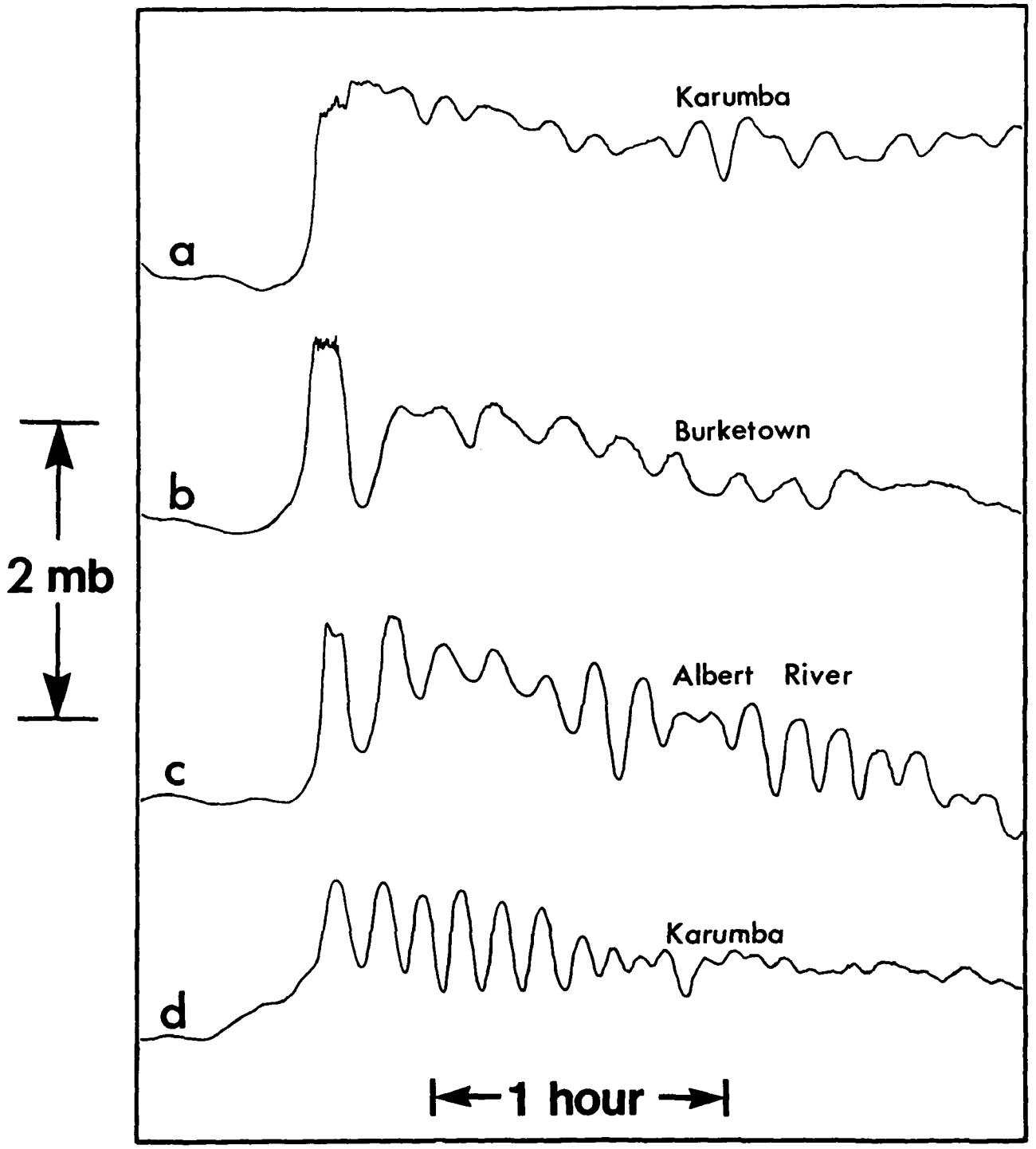

Figure 2

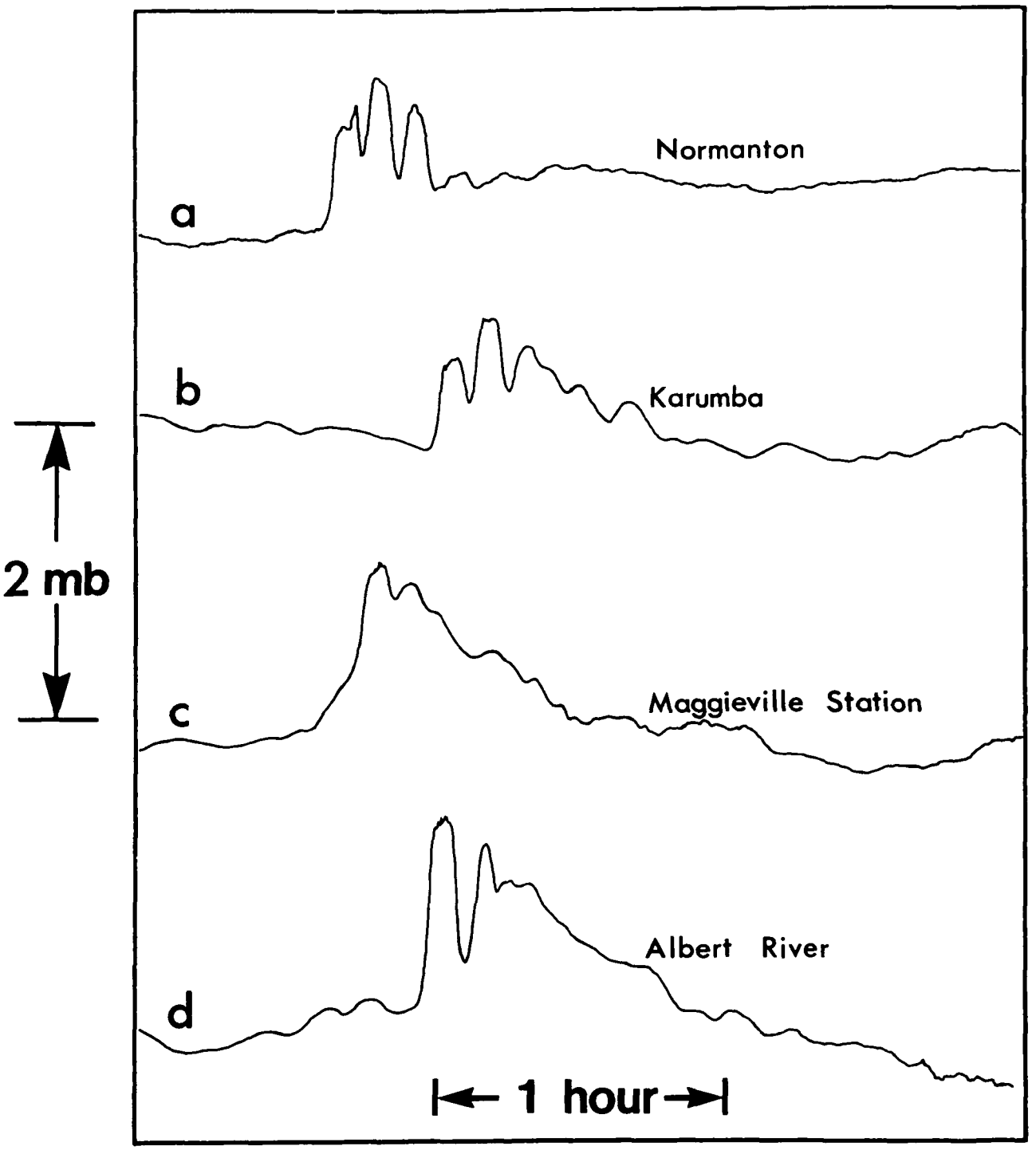
Normanton
a
b
Karumba
2 mb
c
Maggieville Station
Albert River
d
1 hour

Figure 3

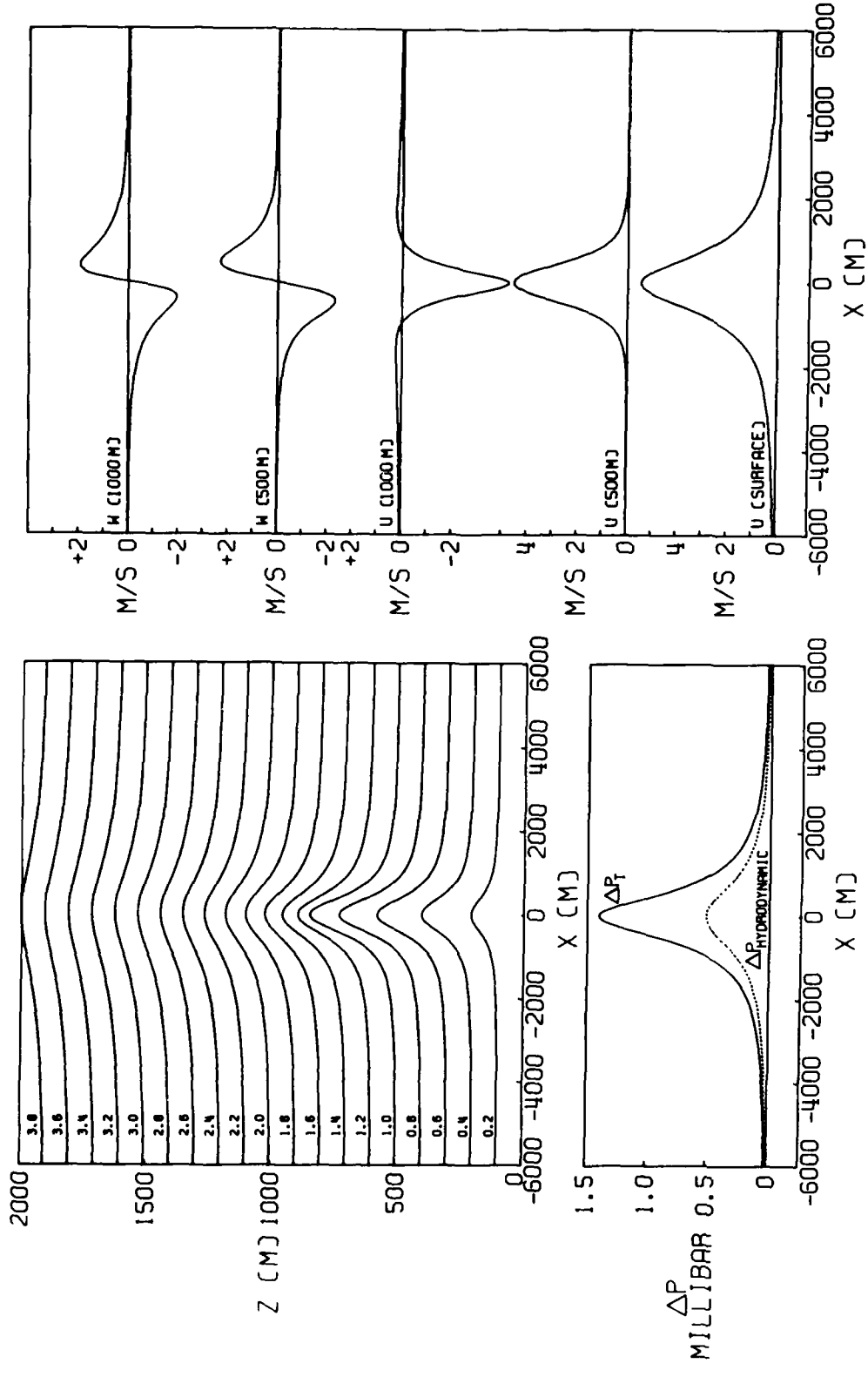
W (1000 M)
W (500 M)
U (1000 M)
U (500 M)
U (SURFACE)
M/S
X (M)
Z (M)
ΔP
MILLIBAR
ΔP_T
$\Delta P_{HYDRODYNAMIC}$

Figure 4

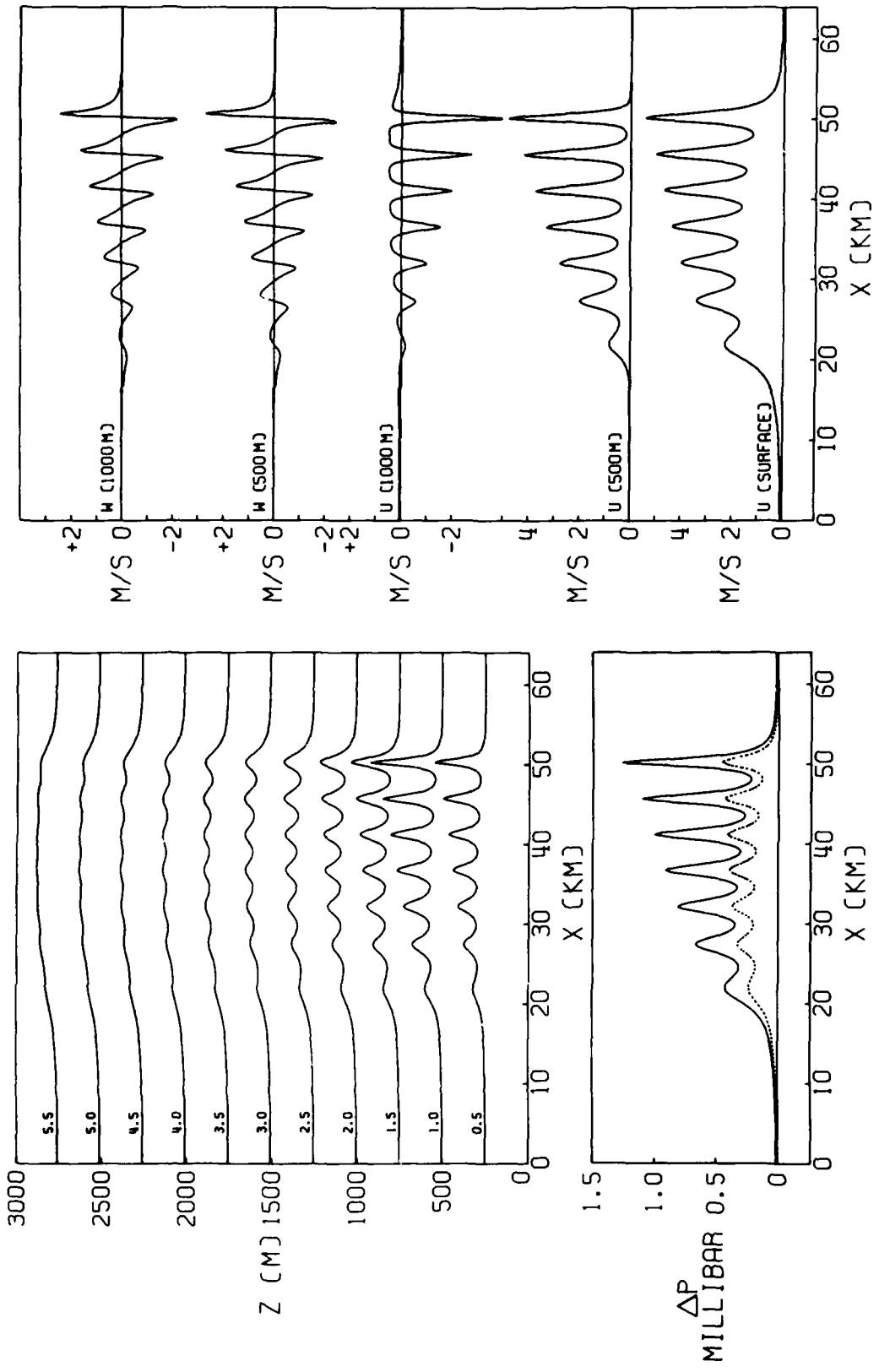

Figure 5

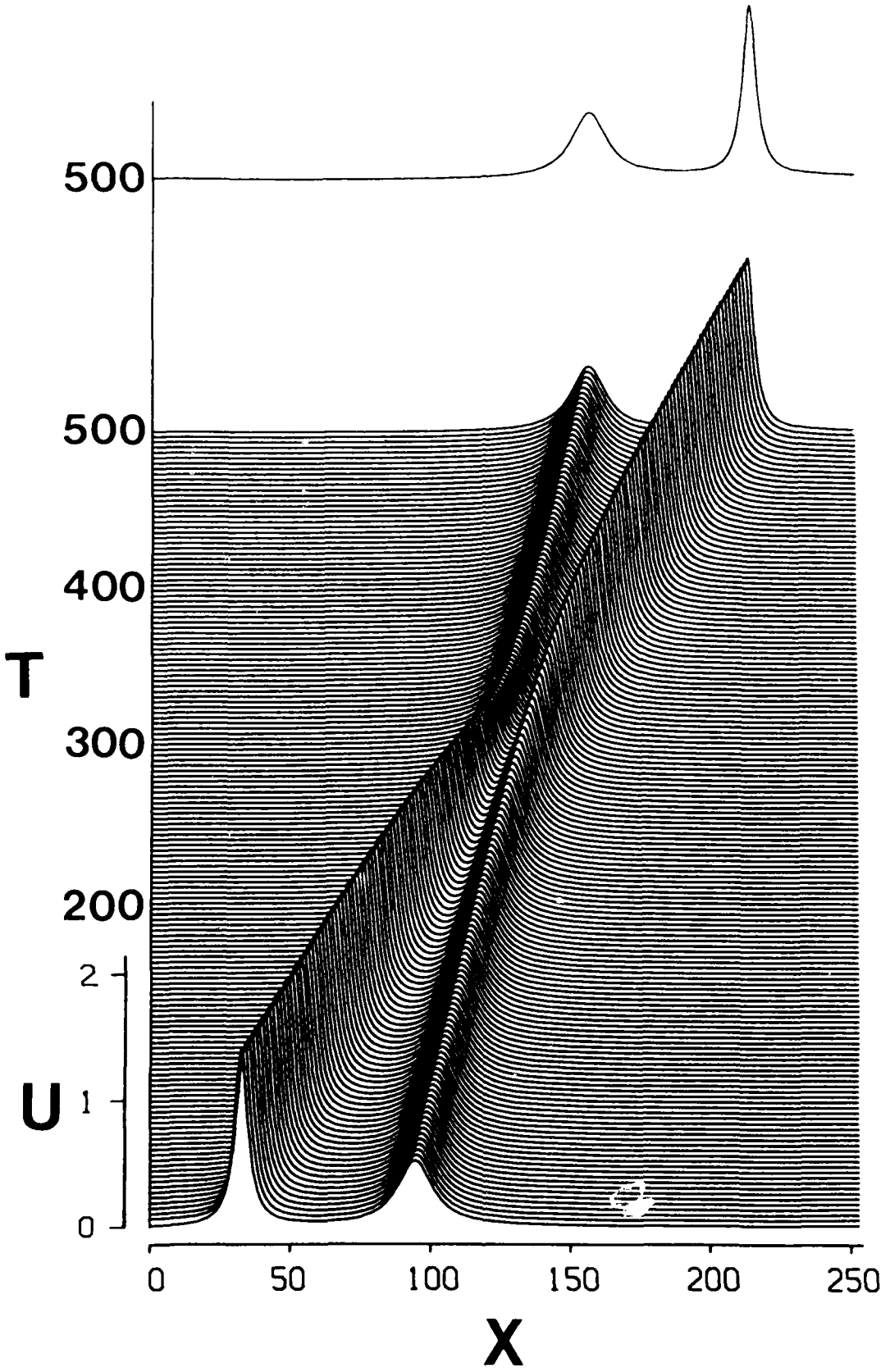

Figure 6

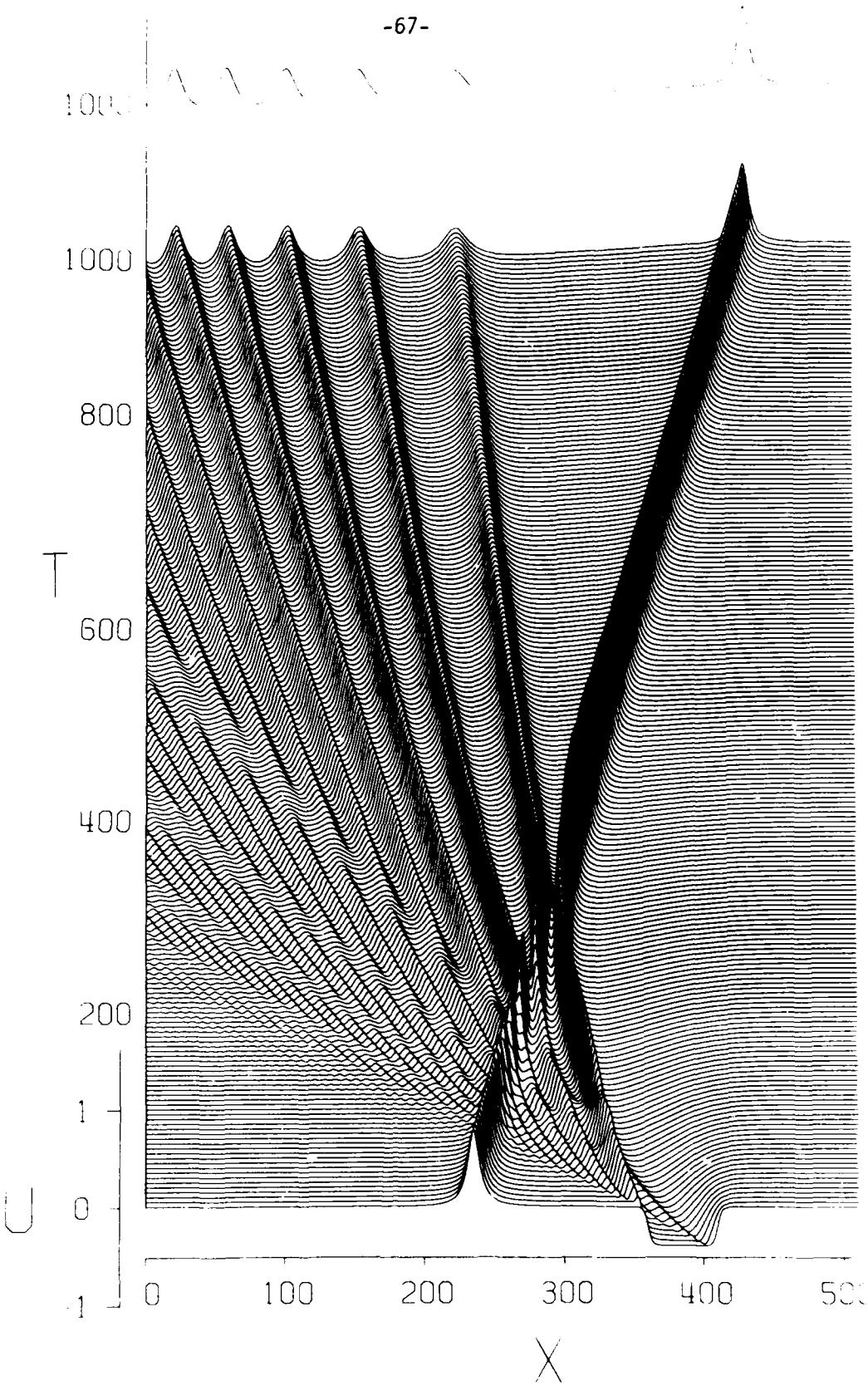

Figure 7

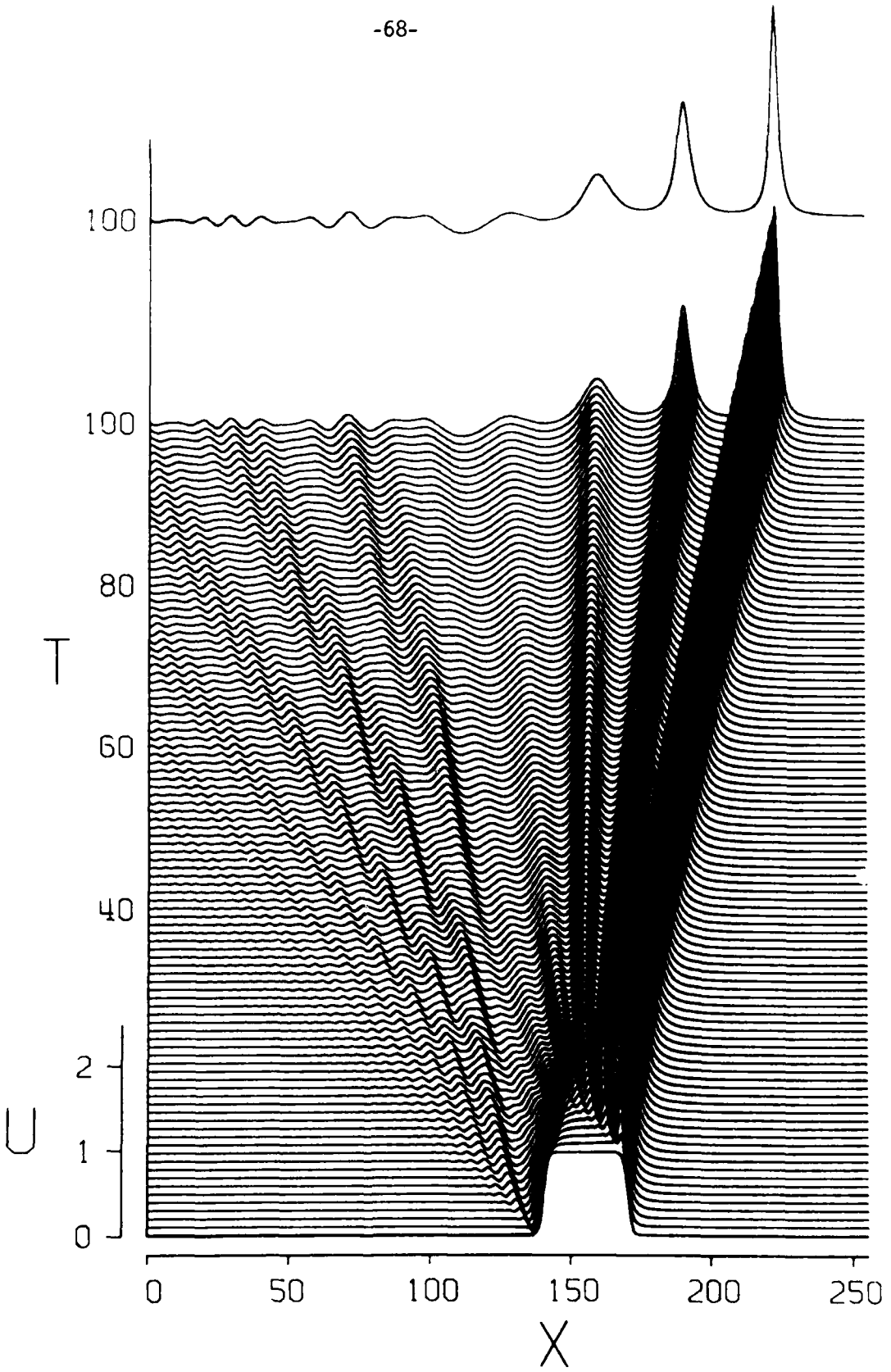

Figure 8

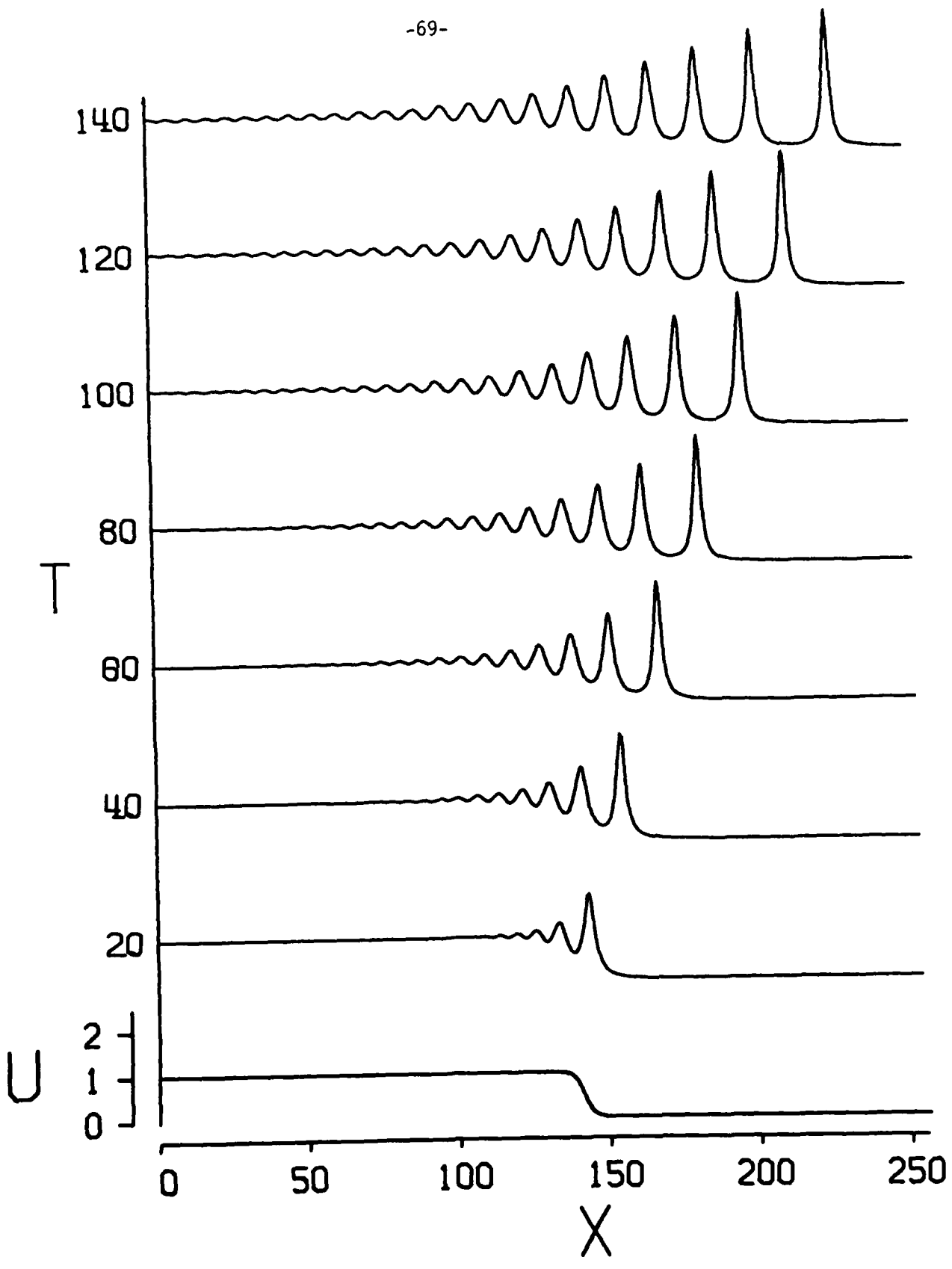

Figure 9(a)

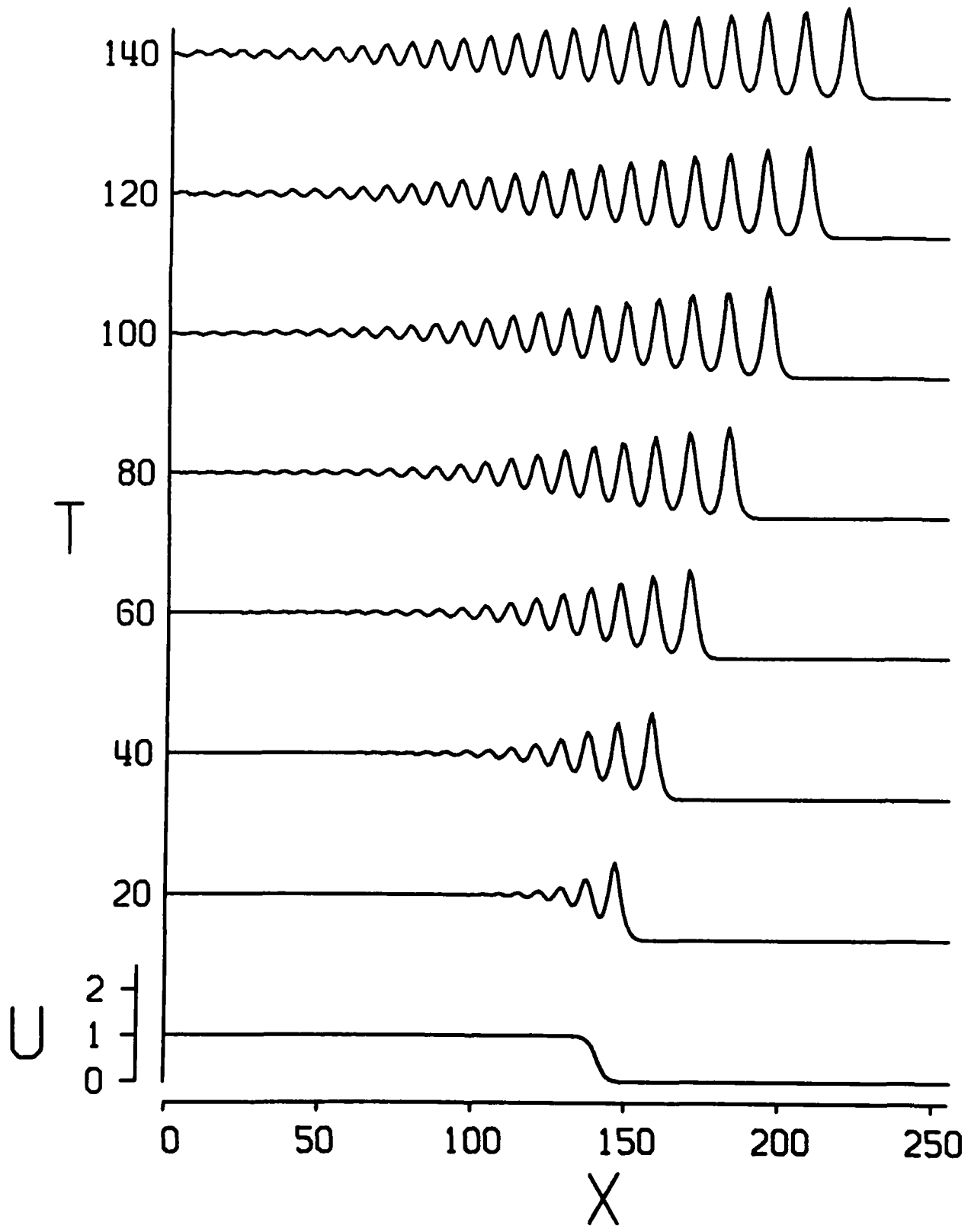

Figure 9(b)

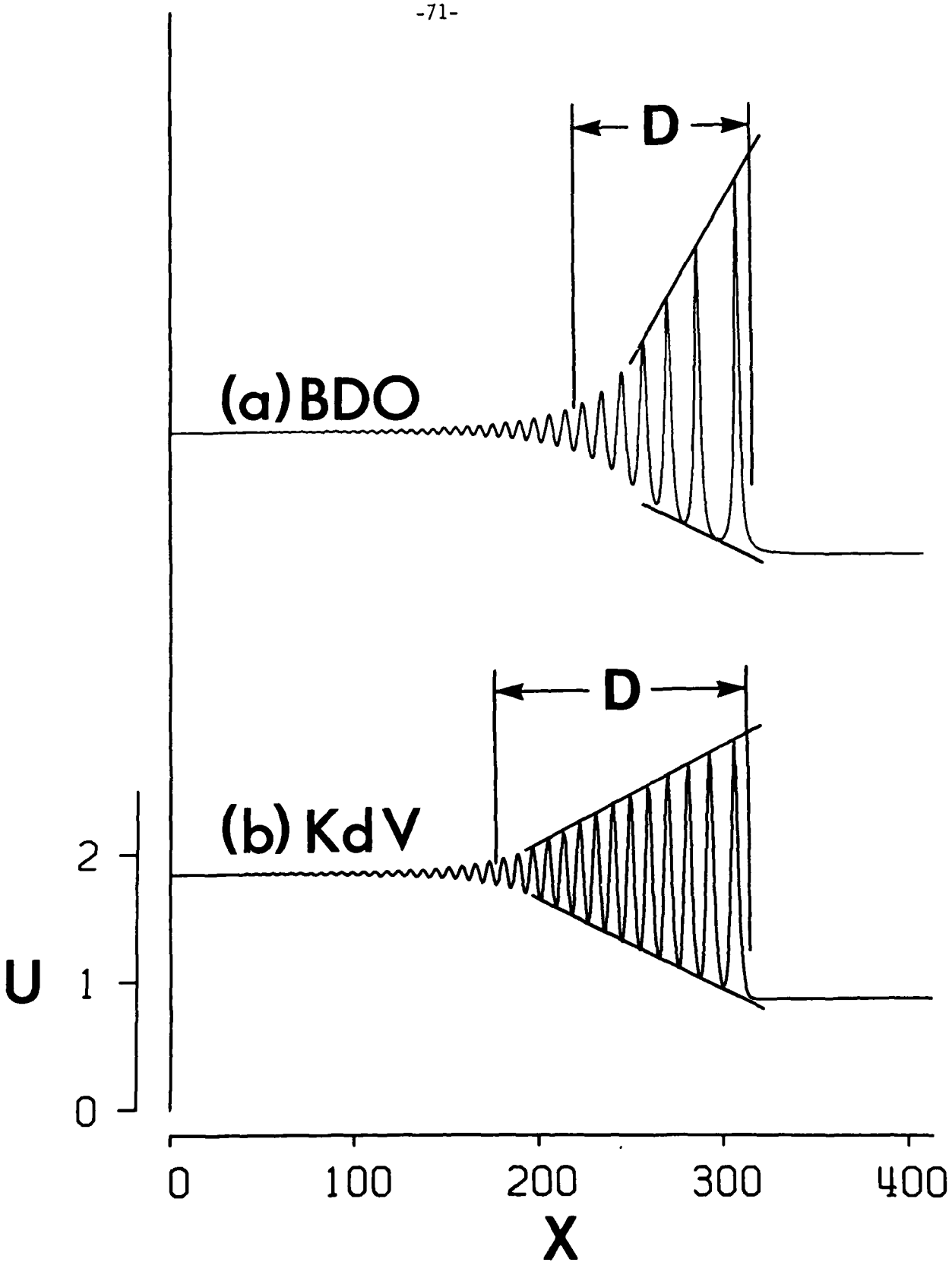

Figure 10

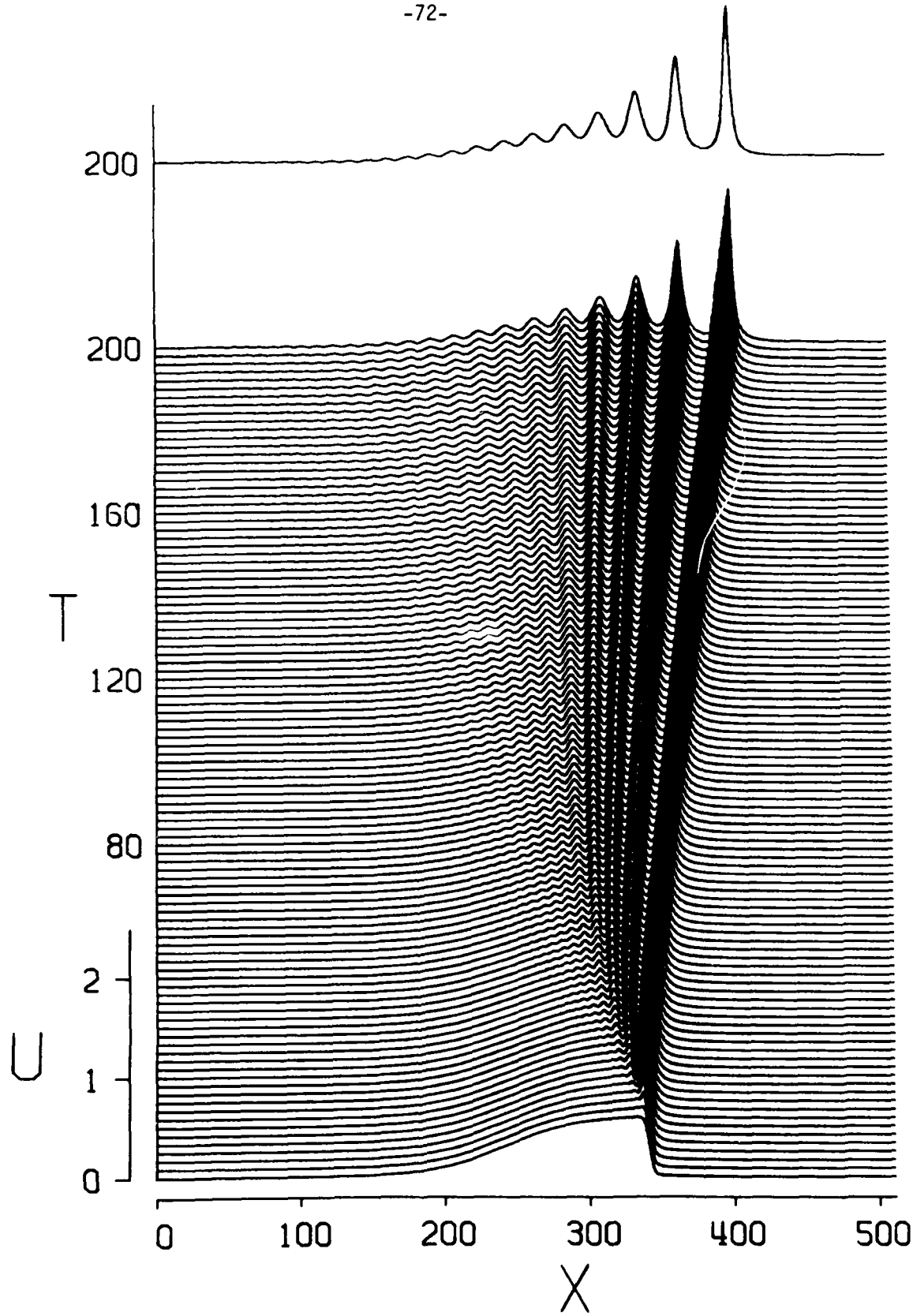

Figure 11

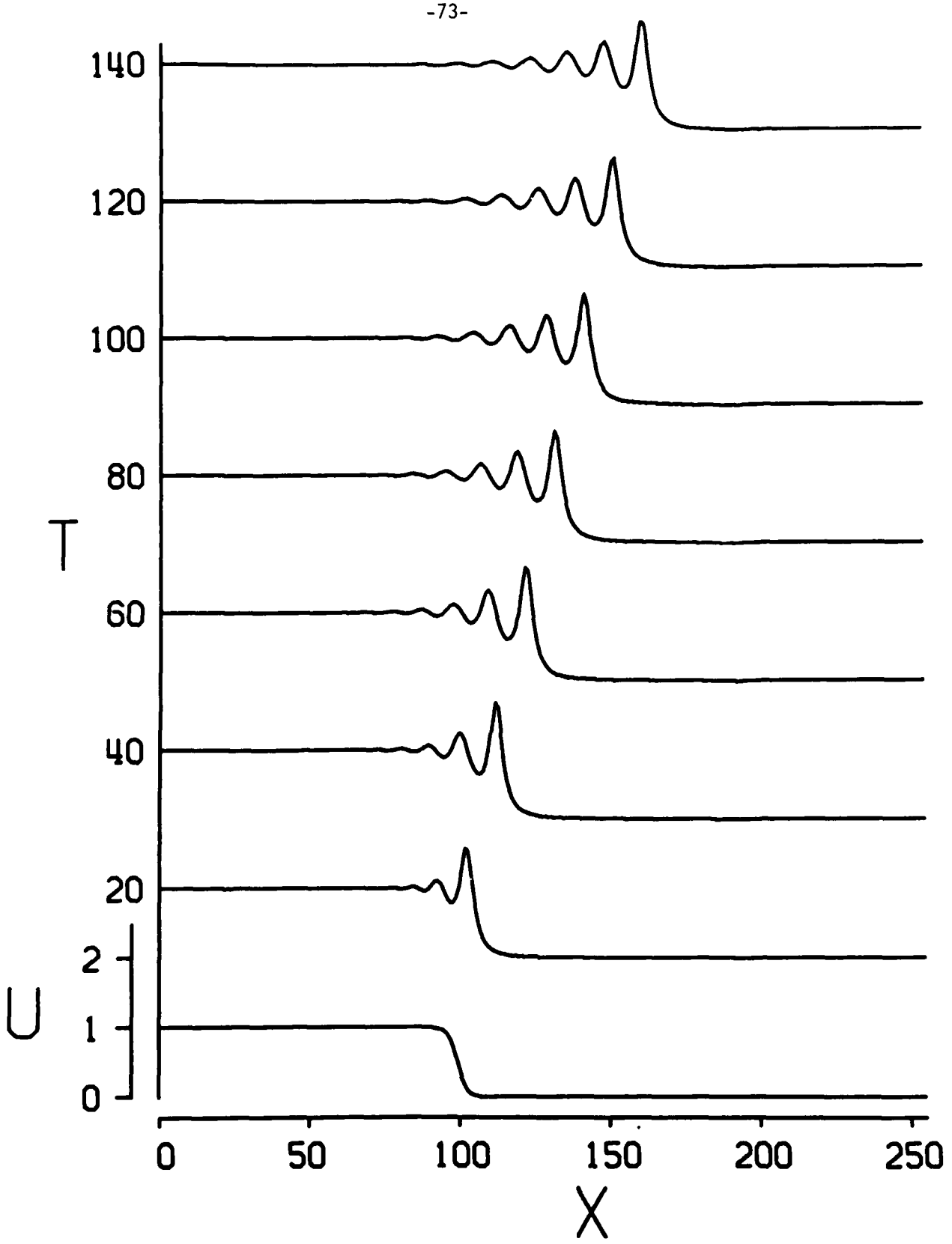

Figure 12(a)

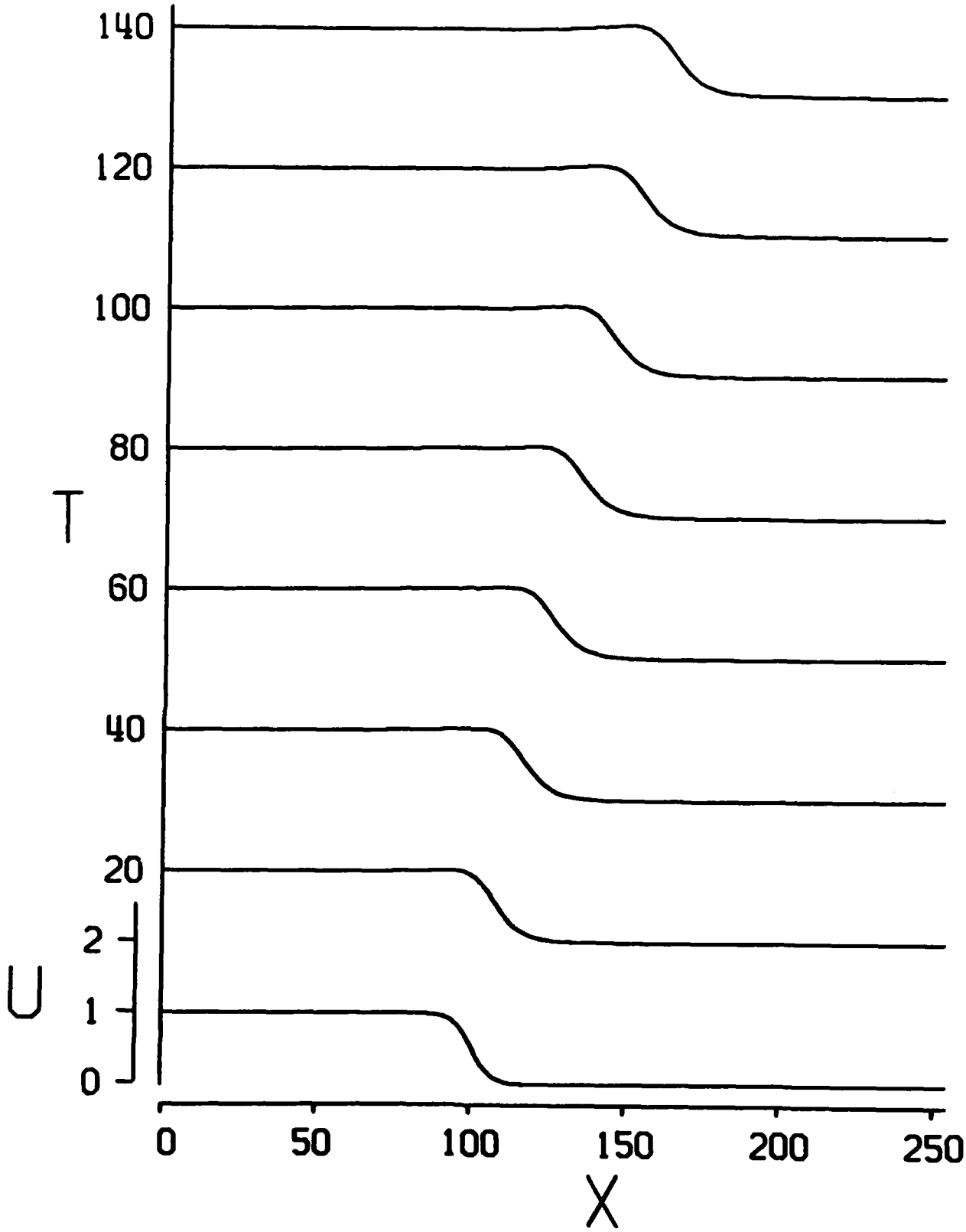

Figure 12(b)

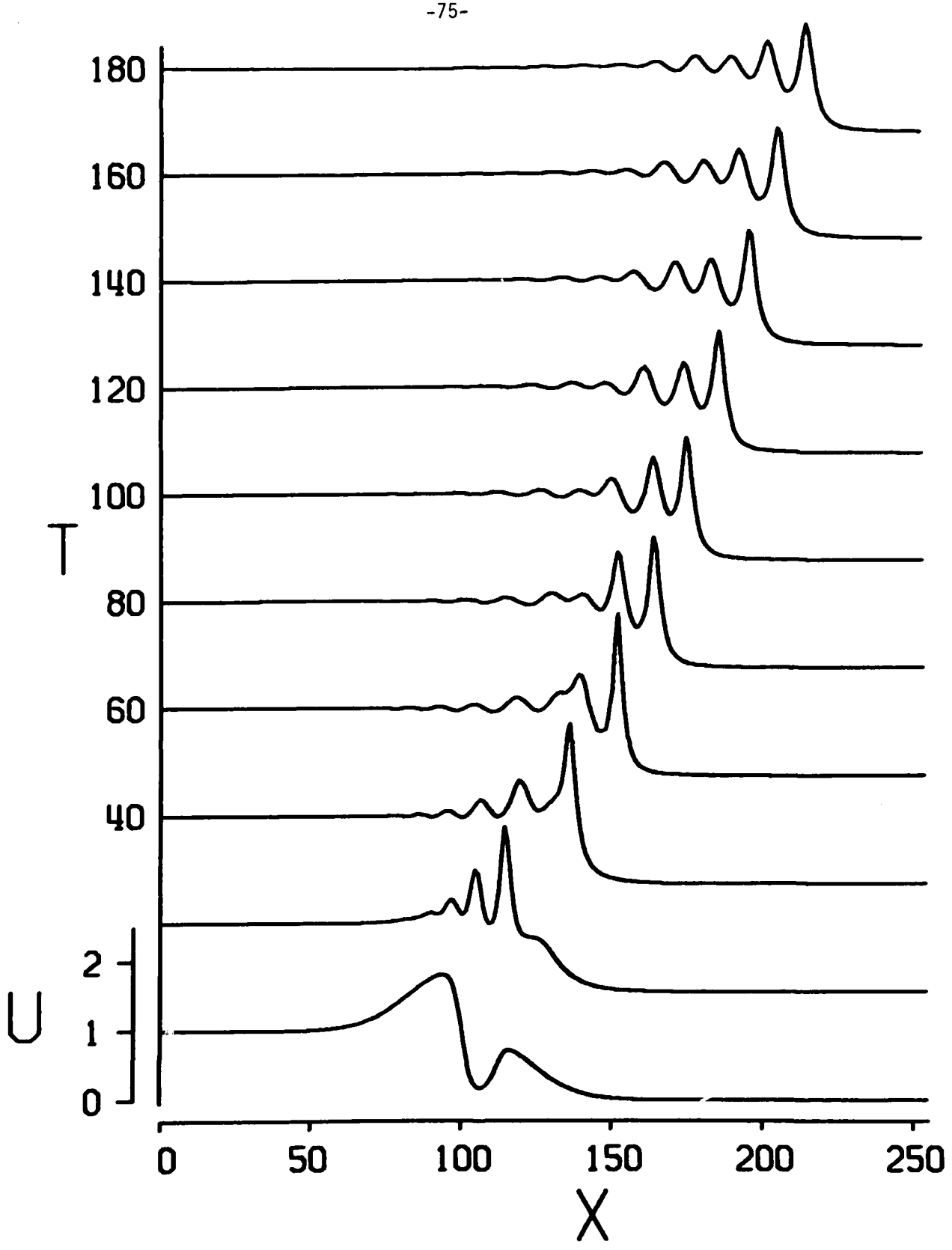

Figure 13

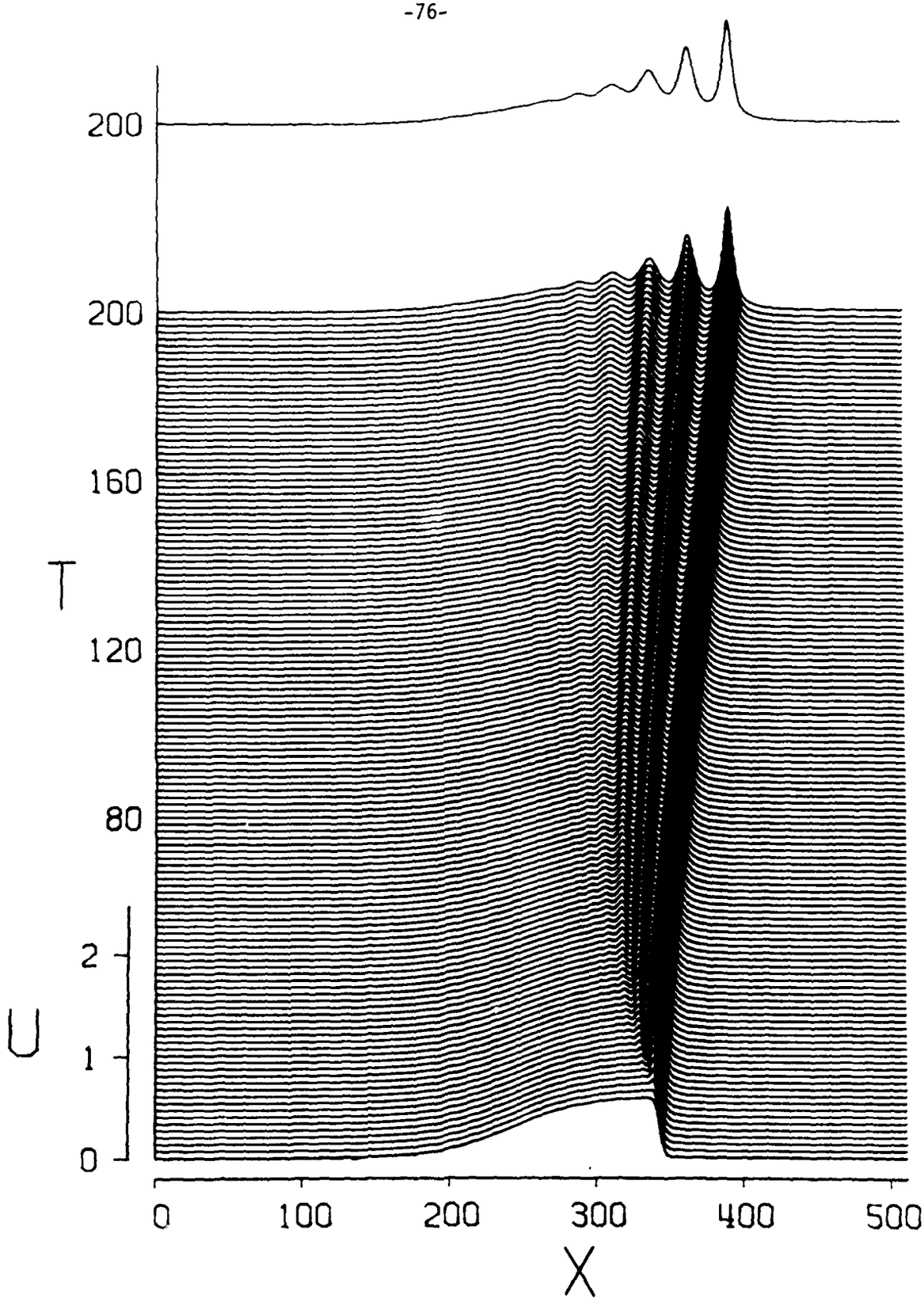

Figure 14(a)

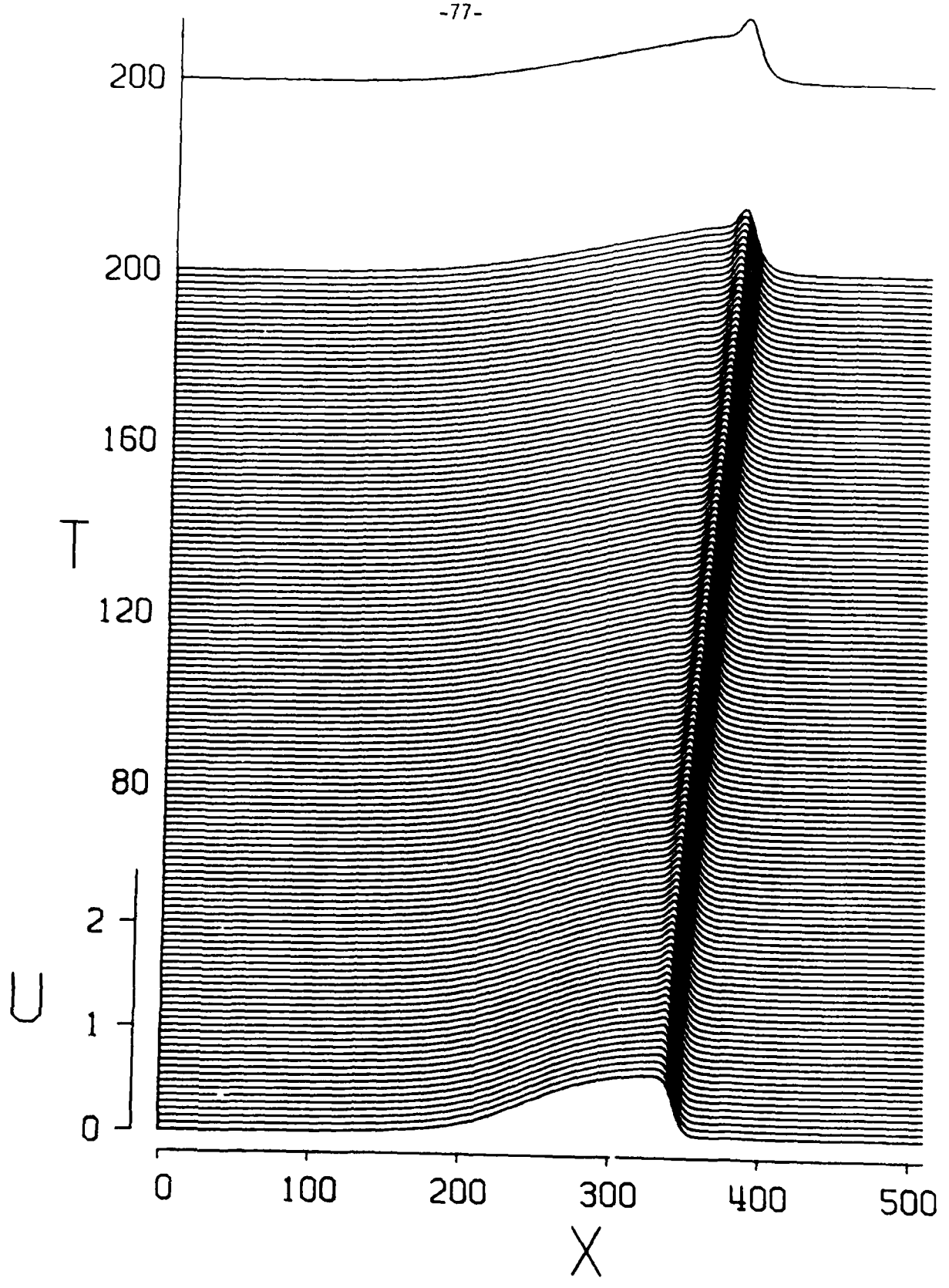

Figure 14(b)

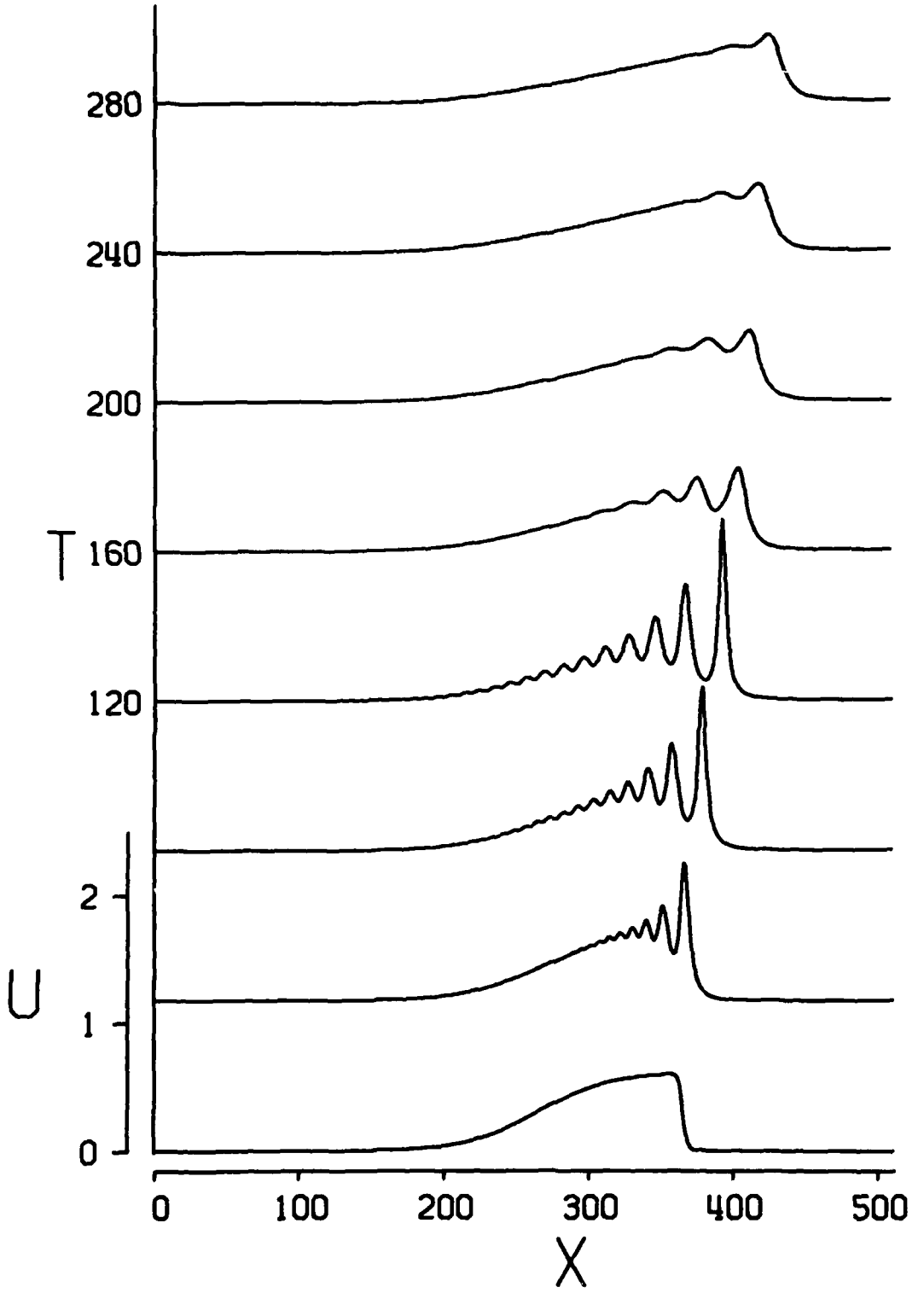

Figure 15

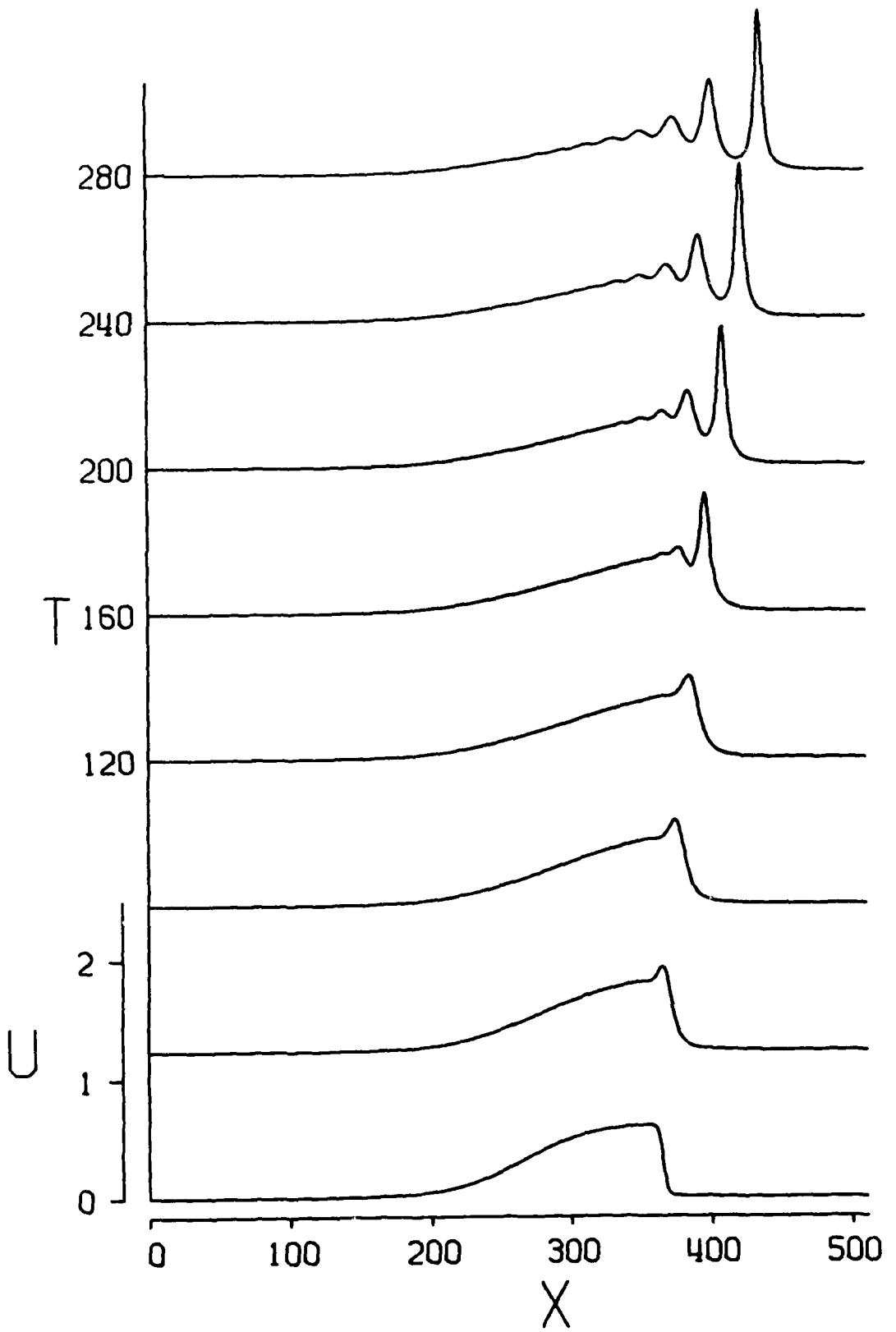

Figure 16

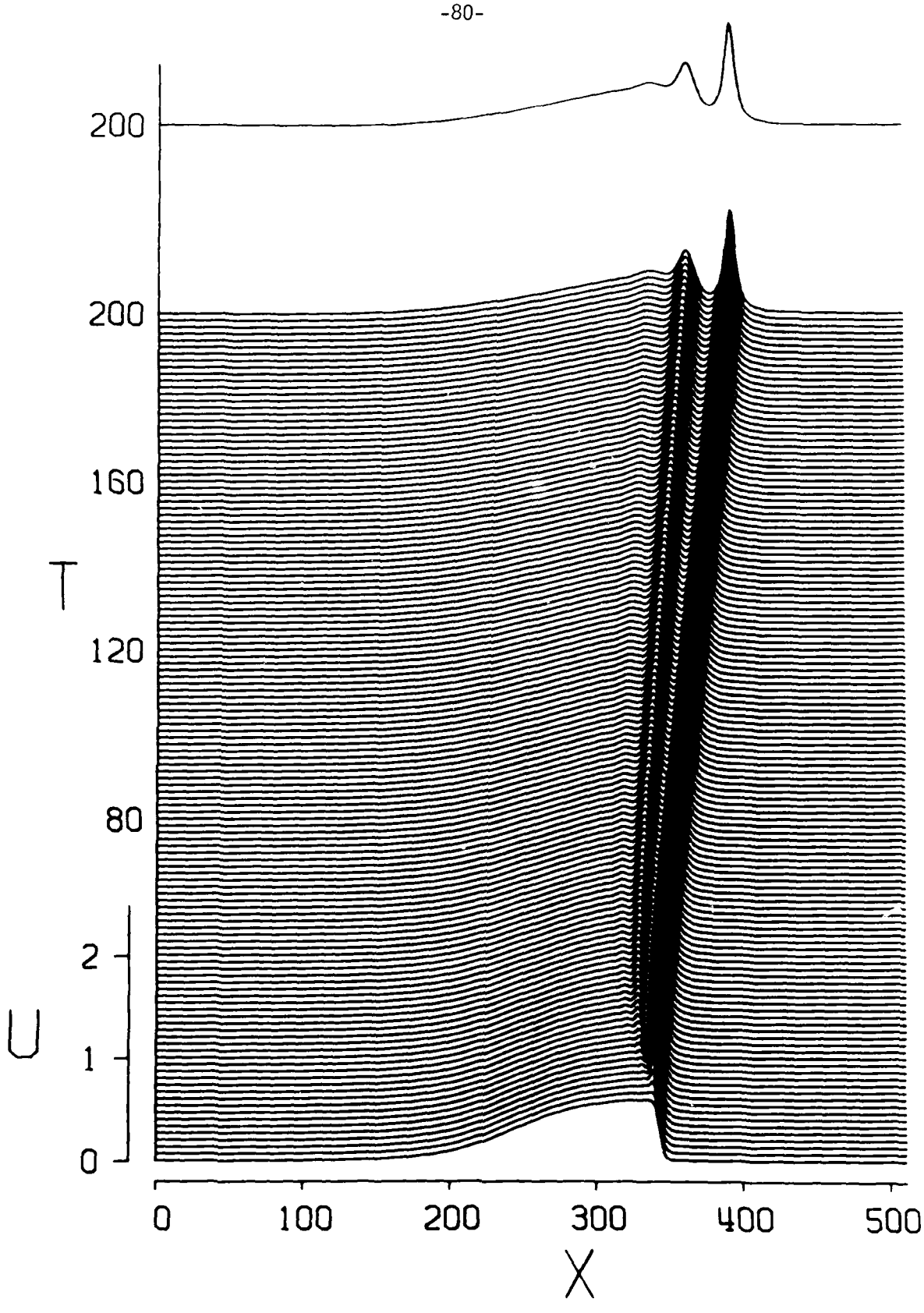
200
200
160
T
120
80
2
U
1
0
0
100
200
300
400
500
X

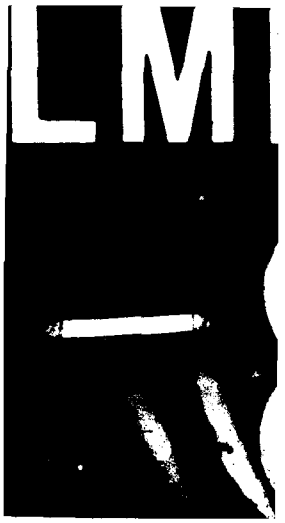
LM